IEEE Access
Multidisciplinary | Rapid Review | Open Access Journal

Received 28 February 2021, accepted 12 March 2021, date of publication 17 March 2021, date of current version 14 August 2023.

Digital Object Identifier 10.1109/ACCESS.2021.3066799

RESEARCH ARTICLE

Solar Power Tower Drives: A Comprehensive Survey

WALEED M. HAMANAH[1], (Student Member, IEEE), ABOUBAKR SALEM[1], (Member, IEEE), M. A. ABIDO[1,2], (Senior Member, IEEE), ABDULAZIZ M. QWBAIBAN[3], (Member, IEEE), AND THOMAS G. HABETLER[3], (Fellow, IEEE)

[1]Department of Electrical Engineering, King Fahd University of Petroleum and Minerals, Dhahran 31261, Saudi Arabia
[2]K. A. CARE Energy Research and Innovation Center (ERIC), King Fahd University of Petroleum and Minerals, Dhahran 31261, Saudi Arabia
[3]School of Electrical and Computer Engineering, Georgia Institute of Technology, Atlanta, GA 30332, USA

Corresponding author: M. A. Abido (mabido@kfupm.eud.sa)

This work was supported by the Deanship of Scientific Research (DSR) at King Fahd University of Petroleum and Minerals (KFUPM) under Project GTEC1701. The work of M. A. Abido was supported by the King Abdullah City's Funding Support for Atomic and Renewable Energy (K.A.CARE), Energy Research and Innovation Center (ERIC) at KFUPM.

ABSTRACT Recently, renewable energy is considered a vital source for electricity generation that aims to reduce the carbon dioxide emissions acquired from fossil fuels. Concentrated solar power (CSP) is a growing technology that collects solar energy from the sunbeams. One of the efficient CSP topologies is the solar power tower (SPT), which aims to collect the direct sunbeams on a central collector using thousands of reflecting mirrors, called heliostats. Many literature reviews have presented the development of control techniques to improve tracking accuracy and SPT performance. However, on the component level, little work has been issued. This article introduces a comprehensive review of the different SPT drives. More than 100 papers have been classified and discussed to allocate the development and the research-gaps in SPT drives. The drive mechanisms, considering both the power source and mechanical transmission systems, have been classified and discussed. Additionally, a comprehensive review of the different electrical motors, along with their power electronic converters, used for heliostat units are presented, discussed, and compared. The advantages and the drawbacks of the different electrical drive systems are presented and discussed. Besides, the azimuth-elevation tracking technique is selected, discussed, and investigated with a dual-axis two linear actuators mechanism. Additionally, a case study for a small-sized heliostat prototype is presented, discussed, and analyzed using the azimuth-elevation dual-axis tracking to investigate the SPT's performance in Dhahran, KSA, as a promising location in the Gulf region. According to this review, the research gaps and future work have been highlighted to help interested researchers in this area finding potential challenges.

INDEX TERMS Renewable energy, concentrated solar power, heliostat control system, electric drives, power electronic converters.

NOMENCLATURE

Abbreviations

CSP	Concentrating Solar Power
SPT	Solar Power Tower
PDC	Parabolic Dish Collector
PTC	Parabolic Trough Collector
LFR	Linear Fresnel Reflector
PV	Photovoltaic
AC	Alternative Current
DC	Direct Current
PMDC	Permanent Magnetic DC
PMSM	Permanent Magnetic Synchronous Motor
PI	Proportional Integration

Symbols

γ^*	reference azimuth angle
α^*	reference elevation angle
γ_{meas}	measurement azimuth angle
α_{meas}	measurement elevation angle
D	Duty Cycle
E_a	back electromotive force
i_a	armature current

The associate editor coordinating the review of this manuscript and approving it for publication was S. Ali Arefifar.

R_a	armature resistance
L_a	armature winding leakage inductance
R_f	field resistance
L_f	field winding leakage inductance
J_m	rotor moment of inertia
B_m	frictional coefficient

I. INTRODUCTION

Nowadays, obtaining a clean environment and reducing CO_2 emissions from fossil fuels has become a significant concern of many researchers. Therefore, most studies focus on renewable energy resources as potential alternatives where the sun is one of the most important renewable energy sources. Solar energy is considered the first option for expanding, upgrading, and modernizing power systems worldwide [1]. Governments all over the world are joining that consensus and preparing their plans in this regard. The usage of renewables is the best option for improving access to affordable, dependable, and more reliable sources of advanced energy services. Around 170 countries have set renewable energy goals, and nearly 150 countries have established policies to capitalize on businesses in renewable energy technologies [2].

One of the promising renewable energy technologies is thermal-based solar power, called the Concentrated Solar Power (CSP) system. The idea of a CSP system's operation is based on gathering sunbeams on a collector that transfers the collected thermal energy using a specific fluid that can be considered a heat source, which can be referred to as a thermal energy generator. This generator can be applied directly to feed thermal systems, like chillers, or indirectly for other applications, such as electrical power generation and water desalination.

One of the preferred CSP technologies is the Solar Power-Tower (SPT) technology that is considered the most efficient among the different CSP technologies. The benefit of SPT topology is flourishing if the commercial development cost is reduced [3]. Consequently, the levelized energy cost for long-term deployment is lower than other topologies [4], [5]. The SPT concept uses a reflector, referred to as heliostats, which reflects sunbeams on a definite point on a collector, referred to as ''target'' placed on the top of the fixed tower. Generally speaking, a heliostat is a flat mirror supported on a movable mechanical structure that tracks the sunbeams using a dual-axis tracking system.

Recently, the work in heliostat tracking and SPT focuses on the tracking systems' control and accuracy and the system calibration. Generally, SPT heliostat fields face the obstacles of high cost and low energy efficiency due to the large number of sensors utilized. A cluster control technique is made to reduce the number of used sensors, reducing the field cost, and achieving reasonable accuracy [6]. Another enhancement is made to increase the SPT overall efficiency by creating multi-reflection stages. This technique provides higher efficiencies. However, the tower receiver's height still needs more investigation [7], [8]. Extensive reviews have been introduced in [9], [10] discussing the current larger-scale SPT systems, concentrating on the tracking error sources and the basic requirements of calibration systems. In addition, the methods for improving power generation efficiency were presented.

Generally, an SPT plant's efficiency depends on the heliostats' ability to reflect the sunbeams on the target [11]. Such reflection over a year requires an accurate drive system to move the heliostat over a wide range of azimuth and elevation angles for precisely reflecting the sunbeams. The precise and reliable drive system needs an expensive power modulator, control system, gearbox, and electric motor. Besides, several thousands of heliostat units are required in one SPT field, which makes the drive system contributing 30–40% of the overall SPT cost [3], [12], [13]. Therefore, the need for an advanced and economic heliostat drive system is essential for SPT technology.

According to the recent work, as far as the authors know, there are gaps related to the SPT heliostat drive systems in the component level considering the electrical motors and the power electronic converters. Therefore, this work introduces a comprehensive survey for the SPT system considering the component level. Hence, this paper presents a review of the most recent CSP technologies and the SPT technology's superiority in terms of system efficiency. The different heliostat drive systems and their constructions will be reviewed. The drive system mechanisms and the electric motors, along with their power electronic conditioners, are described and discussed. A comparison among different drive systems in terms of their cost and performance is presented.

The remainder of this paper is arranged as follows. An extensive survey of the different electric drive systems implemented globally in different SPT plants is introduced in Section I to reflect the current solar energy markets' current situation. A distinct review of CSP systems' topologies and the contemporary world CSP projects are summarized and provided in Section II. The SPT definition and its components are presented in Section III. The drive mechanisms and the power source for the SPT heliostat unit are discussed in Section IV. Section V describes the dual-axis tracking models for the SPT heliostat unit. The electric drive systems, including the different electric motors and their power electronic converters, are discussed in Section VI. Furthermore, in Section VII, a case study of a roof-top small-size heliostat is discussed. Based on the discussions in this review, the authors highlighted the future works in Section VIII. Finally, the conclusion is derived in Section IX.

II. CONCENTRATED SOLAR POWER (CSP)

Scientists classify the sunbeams arriving at earth into three different categories, as shown in Figure 1. These are direct, reflected, and diffuse radiations. The most well-known and efficient solar systems technologies utilize direct and reflected solar radiations such as Photovoltaic (PV) and the CSP systems.

CSP technologies can be classified according to the method of sunbeams concentration to point- and

TABLE 1. CSP projects topologies around the world with the total generation.

Country	No. of Projects	Technology				Power Generation capacity (MW)				Operation (MW)	Under Development and Construction (MW)	Total (MW)
		SPT	PDC	PTC	LFR	SPT	PDC	PTC	LFR			
Spain	50	3		45	2	50		2223.6	30.4	2304	0	2304
USA	24	3	2	18	1	492	3	1257.8	5	1743.8	14	1757.8
China	23	12		7	4	956		464	200	220	1400	1620
India	10	1		7	2	2.5		379	139	228.5	292	520.5
Morocco	7	1		4	2	150		383	2	535	0	535
South Africa	7	2		5		150		450		500	100	600
Australia	5	4			1	155.6			3	2.6	156	158.6
Chile	4	4				1210				0	1210	1210
Italy	3			2	1			5.35	1	6.35	0	6.35
UAE	3	1		2		100		700		100	700	800
France	2				2				21	9	12	21
Israel	2	1		1		121		121		242	0	242
Saudi Arabia	2			2				93		0	93	93
Algeria	1			1				20		20	0	20
Canada	1			1				1.1		1.1	0	1.1
Denmark	1			1				16.6		16.6	0	16.6
Egypt	1			1				20		20	0	20
Germany	1	1				1.5				1.5	0	1.5
Greece	1	1				52				0	52	52
Kuwait	1			1				50		50	0	50
Mexico	1			1				14		0	14	14
Thailand	1			1				5		5	0	5
Turkey	1	1				1.4				1.4	0	1.4
Total	152	35	2	100	15	3442	3	6203.45	401.4	6006.85	4043	10049.85

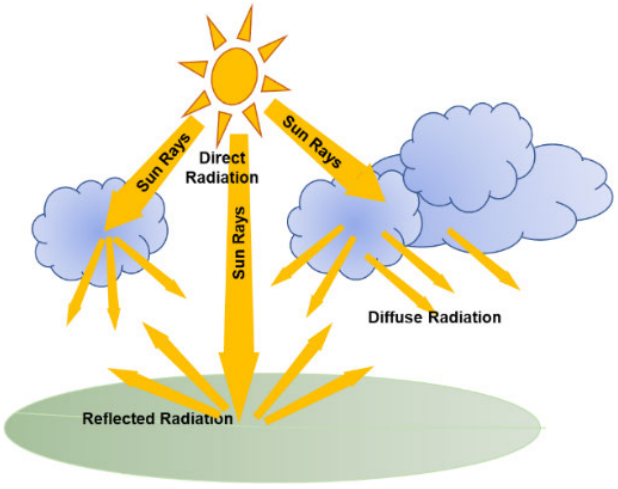

FIGURE 1. Different types of solar radiation.

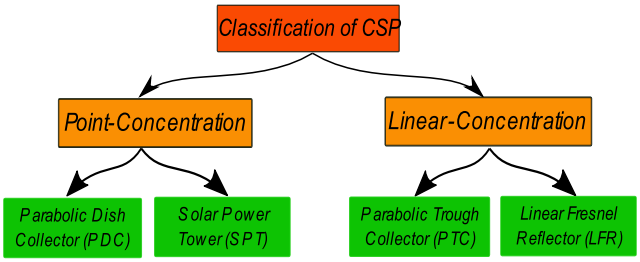

FIGURE 2. Solar energy system classification according to the sunbeam concentration technique.

line-concentrations, as depicted in Figure 2. Two well-known topologies are based on the online concentration: Parabolic Trough Collector (PTC) and Linear Fresnel Reflector (LFC). Conversely, two different topologies are based on point concentration, which is Solar-Power Tower (SPT) and Parabolic Dish Collector (PDC) [14], [15]. The line concentration technique is based on collecting direct solar radiation to collectors, which carry moving fluids that transfer the stored thermal energy to a storage tank. In contrast, the point concentration is based on reflecting the sunbeams to a central target, which can transfer thermal energy to a fluid that can be used as a source of energy. Generally, the point focusing technique is more efficient since it can produce a higher temperature than the line focusing one [16], [17]. The CSP projects worldwide started to appear in the last few years due to advancements in manufacturing. Table 1 provides information for the current CSP plants around the world [18]. The countries are arranged according to the number of projects. This table describes the number of the different CSP projects, the amount of power generated from each type, and the overall generated power. Figure 3 shows the pie-chart representation for the total projects implemented for each CSP technology around the world. Besides, Figure 4 shows a pie-chart representation of each CSP technology contribution to power generation in the world. The different topologies of CSP are briefly described in the following sections.

Firstly, SPT, shown in Figure 5(a), is also known as central receiver systems (CRS). A heliostat field collector (HFC)

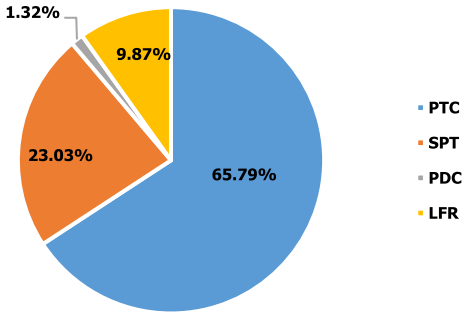

FIGURE 3. Projects of the different CSP technologies.

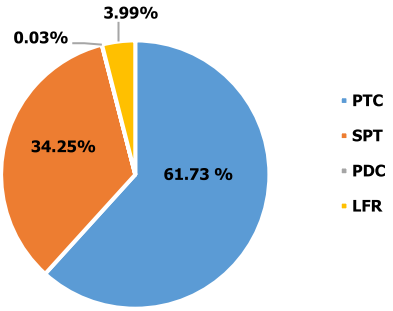

FIGURE 4. Percent generated power for the different CSP technologies.

reflects and concentrates the sunbeams onto a central collector placed on a tower. A heliostat unit is a flat mirror or multi flat mirrors supported by a mechanical structure that follows the sun movement using a dual-axis tracking system. The heat is absorbed by a heat transfer fluid, which then transports thermal energy by heating exchangers that empower a steam Rankine power cycle [19]–[21]. The SPT system produces relatively high temperatures, i.e., 540–840 °C, capable of generating high-pressure steam to move the turbines. Therefore, the cost of thermal storage is reduced substantially [22]. The SPT can be joined with steam cycles with a thermal system efficiency of 40% and can be increased, by the combined cycle, to reach 55% [11]. It could be observed that overall, the share of SPT projects has increased during the last decade compared to other CSP projects in 15 countries, with 53 plants generating around 3442 MW [18].

A simple block diagram for PDC technology is shown in Figure 5(b). PDC system concentrates the sunbeams at a point held above the center of the PDC frame. The whole system continuously tracks the sun movement by moving the collector dish and focal receiver point in all daytime. PDCs systems provide high transformation efficiency compared with other CSP systems. However, they are costly and possess low compatibility concerning storage systems and the hybridization processes [23]–[25]. So, only two PDC projects were established in the USA, and they are out of service. In fact, PDC constitutes only 1.32% of the total CSP projects [18].

Producers claim that PDCs systems can supply mass production, which will allow them to compete with larger CSP

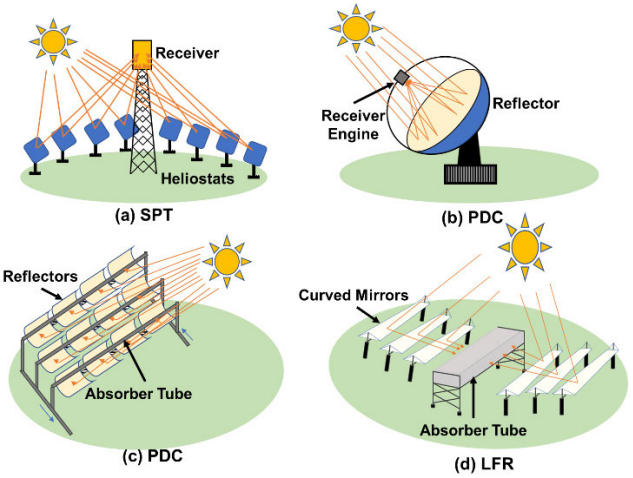

FIGURE 5. Different CSP topologies.

systems. Each PDC system produces electricity independently and offers a low power capacity and usually reaches tens of kW or smaller [26]. Therefore, hundreds of thousands of these dishes are needed to establish a large-scale power station like other CSP topologies with operating temperatures achieved are in the range of 100–1500 °C.

A block diagram for the PTC is shown in Figure 5(c). The PTC reflectors are designed in a curve shape in one dimension to concentrate sunbeams onto the collector tube positioned in the PTC unit's focal line. The movement for both reflector and absorber tube is compatible with the sun for all daytime. That was a group of parallel-connected mirrors called the solar field. The temperature of the PTC varies between 150–400 °C. The PTC can be joined to steam cycles to generate electricity up to 500 MW with a thermal-cycle efficiency of 30–40% [27], [28]. Besides, PTC projects are located in 17 countries, constituting around 23.03% of the overall CSP plants and producing 61.73% of electricity generated by CSP plants [18].

The LFR design approximates the parabolic curve using flat mirrors in long rows to reflect the sunbeams onto a facing direct linear receiver. A receiver is fixed over a mechanical structure, as shown in Figure 5(d), along with the linear reflectors. LFR systems have low installment costs compared to other CSP technologies [29]. However, LFR stations are less efficient than PTC and SPT, and they possess more complexities to connect their storage capacity into the whole design. Recent LFR plants are known as compact LFRs, where two parallel receivers are used with each row of reflector mirrors [30], [31]. Therefore, they require less land than PTC plants with the same output generation, with possession of a high operating temperature range to 150–270 °C. The LFR technology comes in third place, where it has been established in eight countries with 15 projects and a full capacity of about 3.99% of the CSP projects electricity generation [18].

The overall comparison for the different topologies is listed in Table 2. It can be observed that the SPT has higher overall

TABLE 2. Comparison of CSP topologies [21]–[25].

Technology	Collectors	Collector Concentrations	Heat Transfer Fluid	Annual solar to electricity efficiency	Focuses type	Practical operation temperature
SPT	Heliostat	3D	Water(W) Melton Salt (MS) Air(A)	20-35 %	Point	300-565 °C (W) 110-700 °C (MS) 300-1200 °C (A)
PDC	Parabolic Mirror	3D	Hydrogen or Helium	20-30%	Point	> 750 °C
PTC	Parabolic cylinder	2D	Thermal Oil	12-15%	Line	150-400 °C
LFR	Flat Mirror	2D	Water	9-11%	Line	150-270 °C

TABLE 3. Basic approaches for heliostat cost reduction.

Components	Cost	Cost reduction by decreasing	Cost reduction by increasing
Mirrors	25%	• Loads, material cost.	• Beam quality, stability.
Structural support	25%	• Loads thermal, the lever arm of loads, material cost.	• Beam quality, the lever arm of material.
Pedestal and foundation	15%	• Loads, the lever arm of loads, material cost.	• Weight, the lever arm of material, form closure.
Drive system, position sensors & Control system	35%	• Position sensors, loads, controls, cabling, actuator cost.	• Reflected area, the lever arm of bearings, intercept.

efficiency and higher temperature levels [32]. However, a central receiver solar thermal power plant's effectiveness depends on the heliostats' ability to reflect the sunbeams onto the receiver. Reflecting the sunbeams for a full year requires a drive system to move the heliostat over a wide range of azimuth and elevation angles, representing a challenge in developing novel, efficient and low-cost drive systems.

III. SOLAR POWER TOWER SYSTEM

Comparing the different CSP topologies gives an advantage to the SPT system in terms of overall efficiency and temperature levels. However, a central receiver solar thermal power plant's effectiveness depends on the heliostats' ability to reflect the sunbeams onto the receiver. Generally, reflecting the sunbeams for a year requires a drive system to move the heliostat over a wide range of azimuth and elevation angles, representing a challenge in developing new efficient and low-cost drive system designs. Heliostats are considered the bulk cost of SPT plants as they contribute about 40% of the power plants' overall cost [33]–[36]. Therefore, reducing the heliostat cost will lead to a substantial reduction in the SPT overall cost. An impressive amount of unconventional heliostat concepts was found so far as surveyed in [1]. The basic idea for the heliostat cost reduction is given in Table 3.

The following sections describe different drive systems with their motors and the power electronic converters due to the drive system's high share of heliostat unit cost. Besides, various drive system mechanisms, operation, and control techniques are discussed along with their pros and cons.

IV. DRIVE MECHANISMS FOR HELIOSTAT UNIT

The drive system mechanism is accountable for managing the position of the heliostat frame. Meanwhile, they are responsible for applying the required torque to rotate the heliostat structure to reflect the fixed target's sunbeam. For improving the accuracy and efficiency of the heliostat movements, a rotation on two axes, azimuth, and elevation is required [37]–[39]. The movement of the heliostat unit and the meaning of the aforementioned angles will be discussed in Section V.

According to the power source characteristics, the transmission solutions differ considerably to fulfill the heliostat's velocity and torque requirements [39]. The following subsections describe the different power sources and transmission systems used in the industry.

A. POWER SOURCES

Concerning power sources, two well-known technologies are being used in heliostat systems: hydraulic and electrical actuators.

1) HYDRAULIC ACTUATORS

Hydraulic actuators are usually associated with high-power applications [40]. The hydraulic system consists of a hydraulic pump connected with a servo-valve related to electronic control and rotary hydraulic motor [41], [42]. Pumps of incompressible oil power the hydraulic actuators. The pressure that the fluid creates moves the cylinders and, in turn, helps to move the connected load. These actuators are satisfied with high-force applications and are customizable to practically any weight. Besides, they are the most powerful actuators on the market and are suitable to work under heavy loads and pressures.

Due to the pressure-producing system's cost and complexity, hydraulic actuation regularly needs many actuators to move the load. Thus, hydraulic actuators are not competitive when the system requires one or a low number of actuators, as in CSP applications. Furthermore, hydraulic systems require costly plumbing, maintenance, and continuous checks. Due to the nature of the product, the possibility of oil leakages is high. Besides, high-temperature environments can cause damage to the overall system if not monitored

diligently [43]. Hydraulic linear actuators are not contained and require numerous external components. For a small application, these may not be the best option. These actuators are hard to control accurately and may suffer from ''stick-slip.''

2) ELECTRICAL ACTUATORS

Electric motors are used in rotary or linear actuators, as shown in Figure 6 [44], [45]. Among the advantages, the possibility to provide a minimal to large power capability with perfect motions and vast controlling performance can be stated. Different kinds of electrical actuators were being used in heliostat systems with various types of motors, DC, and AC, which were utilized to minimize the driving system cost and increase the system efficiency and controllability. Moreover, lifetime and maintenance characteristics are advantageous as well. These Electrical actuators have much more advantages over hydraulic actuator solutions [46], [47] like:

- Faster response time with higher stability at a wide range of speed control,
- Smoother acceleration and deceleration,
- They are easily programmed for controlling speed and braking.

Hence, the electrical actuator is preferred instead of the hydraulic one, particularly with small-sized heliostat units [48], [49].

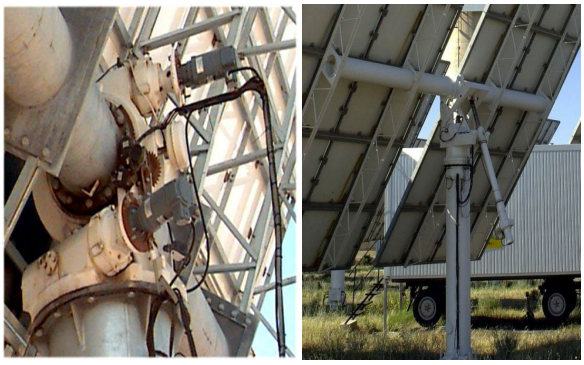

FIGURE 6. Rotary and linear actuators based on electrical actuators.

B. TRANSMISSION SYSTEMS

Several solutions were utilized to achieve the requisite transmission in heliostats [53] depending on the power source, speed, and desired accuracy. Figure 7 shows several gearbox solutions used in various industrial applications. There are some well-known transmission solutions used in heliostats. Besides, the advantages, drawbacks, and applications for each transmission system are listed in Table 4.

1) WORM CONFIGURATION GEARS

Worm gear transmission is shown in Figure 7(a). This gear provides a high transmission ratio in each stage [51]. However, worm gears are not efficient compared to other gearboxes.

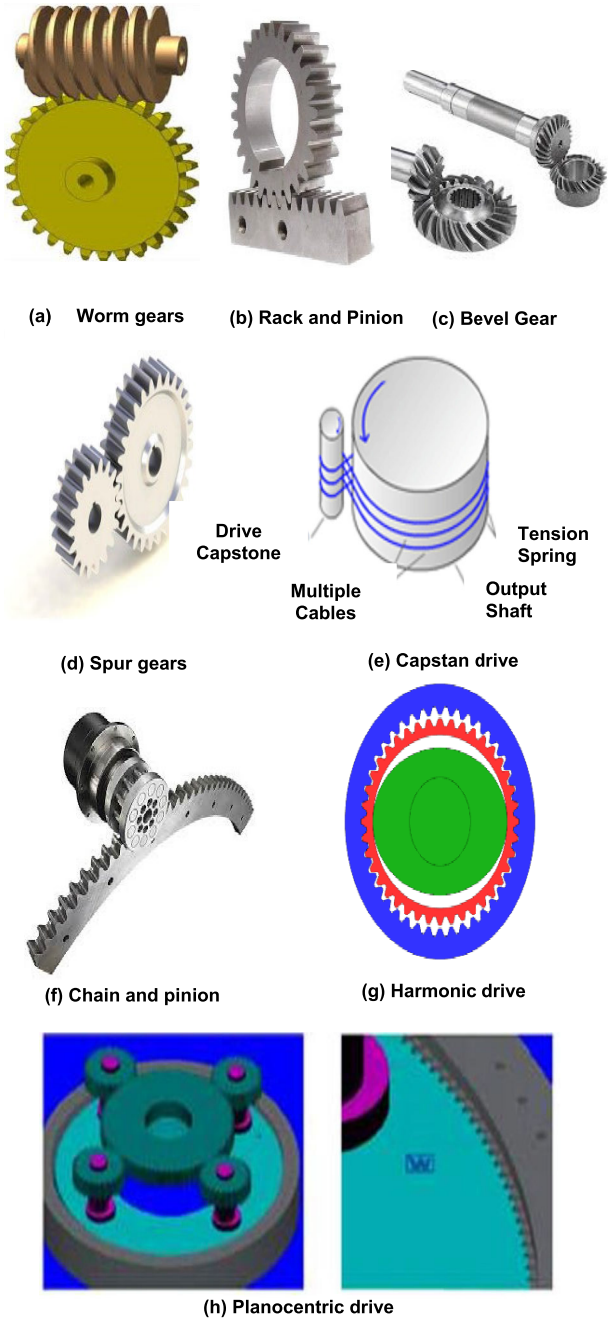

FIGURE 7. Transmission configuration solutions [39].

2) RACK AND PINION GEARS

Figure 7(b) shows the Rack and Pinion gear type. This configuration provides high efficiency with a drawback in transmission ratio, and back driving the stage is always possible [52].

3) BEVEL GEARS

Bevel gears are useful when the direction of a shaft rotation needs to be changed. They are usually mounted on shafts that are 90 degrees apart but can be designed to work at other angles as well, as seen in Figure 7(c). If ball screws

TABLE 4. Advantages and drawbacks for the different mechanism solutions.

Solution	Advantages	Disadvantages	Applications
Worm Gear, [59], [60]	• operate silently and smoothly, • self-locking, occupy less space, • good meshing effectiveness, • used for reducing speed and increasing torque, • the high-velocity ratio of 100:1 can be obtained in a single step	• worm gear materials are expensive • worm drives have high power losses and low transmission efficiency • Produce a lot of heat	• gate control mechanisms • hoisting machines • automobile steering mechanisms • lifts, conveyors, presses
Rack and Pinion, [59], [61]	• cheap, compact, robust, • the easiest way to convert rotary motion into linear motion, more comfortable and more compact control over the vehicle	• less efficiency, • too high a friction, • need replacement frequently	• railway and steering system of cars • in some scales to turn the dial that displays the weight
Bevel Gear, [62]	• able to change the operating angle • differing of the number of teeth (effectively diameter) on each wheel allows mechanical advantage to be changed, • possible to increasing or decreasing the ratio of teeth between the drive and driven wheels, • the rotational drive and torque of the second wheel can be changed concerning the first, • able to increase speed and decrease torque or decrease speed and increase torque	• one wheel of such gear is designed to work with its complementary wheel and no other • must be precisely mounted • the shafts' bearings must be capable of supporting significant forces	• light and heavy truck, • railroad engines, • construction equipment, • aviation, • industrial gearbox, • submarine transmission
Spur Gear, [63], [64]	• constant velocity ratio, • highly reliable, simplest • most comfortable to design and manufacture, • more efficient, and the teeth are parallel to its axis. Hence, a spur gear train does not produce axial thrust. So, the gear shafts can be mounted easily using ball bearings. • used to transmit a large amount of power (of the order of 50,000 kW)	• slow-speed gears, • gear teeth experience a large amount of stress, • cannot transfer power between non-parallel shafts, • cannot be used for long-distance power transmission, • noisy when operating at high speeds	• metal cutting machines • power plants, and marine engines • fuel pumps and washing machines, gear motors, and gear pumps • rack and pinion mechanisms, material handling equipment • automobile gearboxes • steel mills, and rolling mills
Capstan Drive, [65]-[68]	• sample gears designed • light: the combined mass of the input and output gears is 1.0 kg • low friction gearing • has theoretically zero backlash • susceptible to impacts on the environment	• cycle life extremely brief (hundreds to a few thousand cycles) • a material breakdown caused by the abrasion between rope fibers • need Maintaining tension to achieve high stiffness • limit performance if not carefully designed and protected	• tendon drives • Bowden cable systems in robotic manipulators, • automated testbeds, and efficient quadruped robots
Chain and Pinion, [69]	• simpler and less costly, and easier to install • do not slip or creep, and used on reversing drives • no power loss due to slippage; so more efficient • compact, and more practical for slow speed drives • operate effectively at high temperatures and wet conditions • do not deteriorate due to oil, grease, sunlight, or age, and withstand chemicals • stretch due to normal wear is a slow process	• cannot be used where the drive must slip • cannot accept much misalignment • usually require frequent lubrication • noisy and can cause vibration within the machine • do not have load capacities or service life characteristics equal to those of gear drives	• overhead hoists • hydraulic-lift trucks • counterweights that require tension linkages
Harmonic Drives, [70][71]	• offer high efficiency, high torque capacity, • compact size, and zero backlashes, • excellent positioning accuracy and repeatability, • high single-stage reduction ratios and high torsion stiffness	• generally suitable for large reductions (30:1 to 320:1) • high elasticity and nonlinear stiffness and damping, Complex design	• they are currently used in the automotive and space industries, in aviation, medicine, automatics, and robotics
Planocentric Drive [72]	• high efficiency, extremely high torque output • low backlash, high power density • compact design, high permissible input speed	• high cost • generate velocity and torque ripples • complex design	• used in low-speed applications, • constructed with a sun gear, • industrial speed reducers

are employed, the smooth movement and efficiency are significant to move in three axes [53].

4) SPUR GEARS

Spur gears transmission technology provides a smooth movement, as shown in Figure 7(d) [54]. The available transmission ratio in each stage is between 2:5 ranges, so many steps are necessary. The gears have high efficiency with the drawback of having irreversible transmission.

5) CAPSTAN DRIVE

Capstan drive uses a cable to couple the movement of dual elements called capstan drive. Figure 7(e) shows this drive that relies on two pulleys. This drive deals with a rope to the lifters at its end. In this technique, the backlash is canceled, where the gear relies on contact forces and is composed of discrete elements [55].

6) CHAIN AND PINION

Chain and pinion actuation provide the possibility to deal with low-cost transmission [39]. Figure 7(f) offers a clear image of the solution. Chain and pinion solutions require different parts for their assembly, which may impact the overall system's accuracy and efficiency.

7) HARMONIC DRIVE

A harmonic drive configuration solution is called strain wave gear [56]. It relies on contact and deformation to offer a high transmission ratio, usually reaches 100:1, with high accuracy, as shown in Figure 7(g). The configuration has high efficiency with a backlash-free rotational motion transmission. However, the high cost prevents its use in CSP applications [57], [58].

8) PLANOCENTRIC CONFIGURATION

Planocentric configuration solution drives implement extraordinary gear reduction reaching over 30000:1 in a very compact package Figure 7(h). The heliostats units are considered the only application for this concept, and they cannot profit from these systems produced for other applications. The solution suggested being the lowest-cost option for large heliostats azimuth heliostats [39].

V. A HELIOSTAT'S DUAL-AXIS TRACKING

To understand the drive system's rule, the tracking system requirements have to be defined in terms of sun and heliostat angles. The solar tracking systems must be adjusted continuously and accurately to reflect the sunbeams. A single-axis tracking system is less costly, and its control system is simple to be achieved. However, system efficiency is less compared with the dual-axis solar tracking system. To track the sunbeams, three sets of angles must be defined, i.e., sun, tower, and heliostat angles. The following subsection describes the mathematical model used to identify these angles.

A. SOLAR MODEL

Two principal angles are needed to define the sun position. These are solar elevation angle (α_s) and solar azimuth angle (γ_s) (See ***Figure 8***). The α_s angle is expressed by:

$$\begin{aligned} \alpha_s &= 90 - \theta_z; \\ \theta_z &= \cos^{-1}\left[\cos(\varphi)\cos(\delta)\cos(\omega) + \sin(\varphi)\sin(\delta)\right]; \\ \delta &= 23.45\sin\left(360 \times \frac{284+n}{365}\right) \end{aligned} \tag{1}$$

where δ is the declination angle, θ_z is the zenith angle, φ is latitude angle, ω is the time angle, and n is the day number; $n = 1$ on Jan. 1st every year.

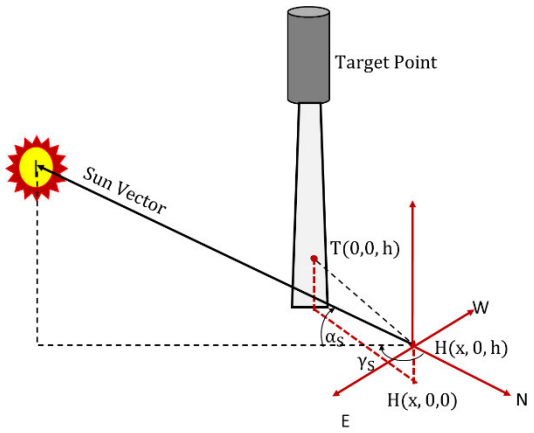

FIGURE 8. Elevation and azimuth sun angles.

The angle δ is the sun's angular position at solar noon concerning the equator's plane, north positive; $-23.45° \leq \delta \leq 23.45°$. The angle θ_z is the angle between the vertical and the line to the sun, that is, the angle of incidence of beam radiation on a horizontal surface. Additionally, the angle $\boldsymbol{\varphi}$ is the angular location north or south of the equator; i.e.$-90° \leq \boldsymbol{\varphi} \leq 90°$ where north is positive. The angle ω is the angular displacement of the sun east or west of the local meridian due to rotation of the earth on its axis at 15° per hour considering morning in negative and afternoon in positive [73], [74]. Depending on time and date values (year, month, day, hour, minute, and second) and location (longitude (φ) and latitude angles), the solar elevation and azimuth angles are described in Figure 8. The angle γ_s can be calculated as:

$$\gamma_s = sign(\omega)\left|cos^{-1}\left(\frac{\cos(\theta_z)\sin(\varphi) - \sin(\delta)}{\sin(\theta_z)\cos(\varphi)}\right)\right| + 180;\ \theta_z \neq 0 \tag{2}$$

It is worth mentioning that this angle's zero value is not achievable, as been proved practically in Section VII.

B. TOWER AND HELIOSTAT MODEL

The tower elevation angle (α_T) which is a function of the tower height (H), the heliostat height (h), and the distance of the heliostat from the tower (R), which is illustrated in Figure 9. In addition to the elevation angle, the target position

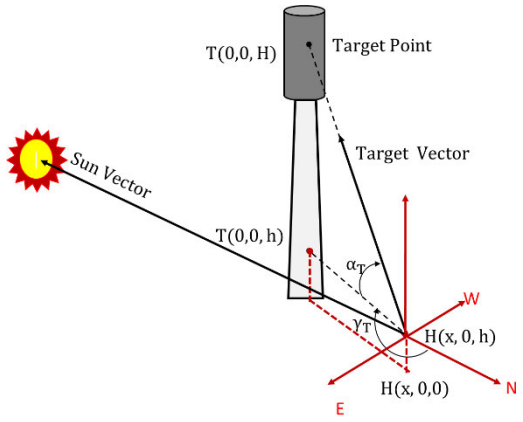

FIGURE 9. Elevation and azimuth target angles.

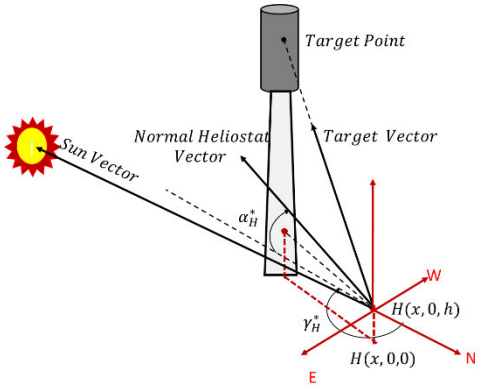

FIGURE 10. Elevation and azimuth heliostat angles.

of the tower is defined by the azimuth target angle (γ_T) which is referenced by the North direction of the heliostat and tower.

The sun tracking is identified by two angles, called heliostat angles, as described in Figure 10. These angles are heliostat elevation angle (α_H^*) and heliostat azimuth angle (γ_H^*). The following method is used to obtain the heliostat tracking angles. Firstly, the sun and tower angles are converted to Cartesian coordinates as described by (3), (4). Then, the normal mirror vector based on three-dimensional Cartesian form (x, y, and z) can be calculated using (5). Finally, the heliostat tracking angles α_H^* and γ_H^* can be calculated using (6) [75].

$$\begin{aligned} z_1 &= \sin(\alpha_s) \\ x_1 &= \cos(\alpha_s) * \cos(-\gamma_s) \\ y_1 &= \cos(\alpha_s) * sin(-\gamma_s) \end{aligned} \tag{3}$$

$$\begin{aligned} z_2 &= \sin(\alpha_T) \\ x_2 &= \cos(\alpha_T) * \cos(-\gamma_T) \\ y_2 &= \cos(\alpha_T) * sin(-\gamma_T) \end{aligned} \tag{4}$$

$$z = \frac{z_1 - z_2}{2} + z_2 \tag{5}$$

$$\alpha_H^* = sin^{-1}\left(\frac{z}{\sqrt{x^2+y^2+z^2}}\right)$$

$$\gamma_H^* = \begin{vmatrix} tan^{-1}(-y/x) & if\ x > 0 \\ tan^{-1}(-y/x) + 90 & if\ x < 0,\ and\ y \geq 0 \\ tan^{-1}(-y/x) - 90 & if\ x < 0,\ and\ y < 0 \\ 90 & if\ x = 0,\ and\ y > 0 \\ -90 & if\ x = 0,\ and\ y < 0 \\ \text{undefined} & if\ x = 0,\ and\ y = 0 \end{vmatrix} \tag{6}$$

VI. ELECTRICAL DRIVES FOR DUAL-AXIS TRACKING SYSTEMS

A block diagram for a generic electrical drive system is shown in Figure 11. It mainly consists of an electric motor, power electronic converter, sensors or transducers, and a digital controller. The power electronic converter is used to modulate the input supply to a suitable energy source for the electric motor. The sensors are used to transfer the measured signals to the digital controller. The control technique is implemented within the digital controller to steer the power electronic converter with a suitable train of pulses suitable for the control command.

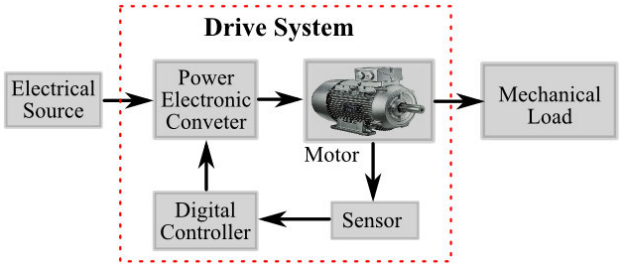

FIGURE 11. Generic block diagram for the electrical drive system.

For a heliostat dual-axis solar tracking system, the mechanical load represents the mirror, the movable structure, and the gearbox coupled with the motor shaft to transfer the mechanical energy to a suitable form; for instance, from rotational motion to translational motion for linear actuators. The sensor needed for such a system is a position sensor that is used to feedback the mirror position measurement. Based on the electrical source nature, AC or DC, and the motor type, the power electronic converter can be selected. On the other hand, motor selection depends on the mechanical characteristics of the connected load. Two-directional movements are needed to control both azimuth and the elevation axes to maximize the reflected solar energy. In the next subsections, the different electrical drive systems will be elaborated.

A. DC DRIVES

DC motors are mostly used in many applications because of their control simplicity at a wide range of speeds, in addition to the ability to operate at high torque values. Moreover, DC motors have the advantages of fast starting, acceleration,

deceleration, forward, and reverse responses. Different DC motors can be used in SPT applications, i.e., shunt, compound, and permanent magnet DC motors [76].

In early 1985, DC drives have been utilized for an old SPT heliostat design, as described in [77], [78]. A switched-mode DC/DC Buck regulator, shown in

Figure 12 is used to drive a Permanent Magnet DC (PMDC) motor [78]. This converter allows a unidirectional power flow that helps only the motoring operation of DC motors. However, the abovementioned circuit cannot control the DC motor in the four quadrants, essential in DC drives. Furthermore, Buck converter is a switched-mode regulator that includes a passive filter, which is unnecessary for drive applications, where the machine inductance fulfills the current filtering.

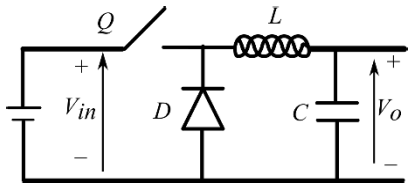

FIGURE 12. Buck DC/DC switched-mode regulator.

In [79], a bidirectional DC/DC converter, Class-E DC chopper shown in Figure 13, is used to supply the armature winding of a separately excited DC motor. This converter topology is preferred in DC drive applications to fulfill the four-quadrant operation, including motoring and reverse motoring. However, the field winding of this DC motor requires an additional DC source to energize the machine.

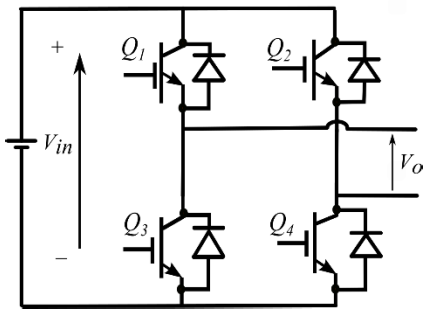

FIGURE 13. Class-E DC chopper.

Regarding the control techniques, neural networks, PI, and PID controllers are commonly used to control heliostat drive systems' movement. The PI and PID gains are tuned using two different fuzzy logic (FL) techniques in [79]–[81]. The two methods are based on considering the error signal and/or derivative of the error signal. The results reflected the FL technique's superiority that felt both the error signal and its derivative. However, these studies have not been experimentally validated. In [82], computer vision is used to control the dual-axis heliostat drive system. An educational prototype is made based on a thermal camera interface to a Raspberry Pi microcomputer system. This system is considered the most advanced in SPT control techniques. However, applying such a method to practical SPT with thousands of heliostat units is not feasible due to the high cost. Although DC drive control is preferred due to its simplicity, the DC drives have the drawbacks of relatively high capital cost and regular maintenance costs due to commutators and brushes' incidence. These are considered a severe issue for CSP plants that have thousands of heliostat units, likewise the Noor III CSP plant in Morocco, which has around 50,000 computer-controlled heliostats or mirrors spread over a 30 km^2 area [83].

For the interested readers, the well-known applications, the advantages, and drawbacks of the different DC motor types are listed in Table 5. Furthermore, brushed DC motors are mainly used in CSP applications requiring high dynamic performance that used drives up to several hundred kilowatts [92], so the different power electronic converters used for brushed DC drives are depicted in Table 6.

B. STEPPER MOTOR DRIVES

Stepper motors (STMs) are prevalent in the heliostat drives units considering their relatively high torque at low speeds. Generally, STMs are classified into three main categories, i.e., variable reluctance STM, permanent magnet stepper motor (PM-STM), and hybrid stepper motor (HB-STM) [96]. A stepper motor's general features are the ability to work at open-loop control and the high precision movement with non-accumulated movement error. Moreover, the absence of a commutator leads to less maintenance and a long lifetime. Therefore, no shaft encoder is needed to acquire the motor position [97].

Currently, STMs are used in the dual-axis tracking system for heliostat drives [98]–[102]. Modeling and simulation of closed-loop control for STMs are presented in [98], where two sets of HB-STM drives are used to control an SPT located in the Sonora desert in Mexico. Although STM operation does not require shaft encoders to define the motor position, it has been used in a closed-loop control to move the heliostat structure, which leads to an increase in the drive system cost. The power electronic circuit used to drive an STM depends on the number of stator phases, i.e., two, three, and four phases of stepper motors [99]. Therefore, the two-phase bipolar stepper motor used in [98] requires two Class-E DC chopper modules, as shown in Figure 14.

Another study in [100] provided an HB-STM for SPT based on using a thermal camera. The image processing along with FL is used to analyze the image in order to track the sunbeams. Accurate experimental results have been obtained. However, the drive system cost and complexity are high due to the thermal camera and the digital controller used for image processing. Furthermore, having thousands of heliostat units, complex interfacing circuits, and multiples of digital controllers can be difficult to deal with.

It is worth mentioning that the unipolar PM-STM, shown in Figure 15, is another configuration for PM-STMs configuration, in which the phase mid-points are commonly connected

TABLE 5. Comparison of the different motors used for heliostat units.

Type of Motors		Advantages	Disadvantages
DC Motor	Permanent magnet [84], [85]	• smaller size, and available in wide ranges of horsepower, • low cost, and no need for field windings, • no rotor copper losses	• the generating capacity of working flux within the air gap is limited, • noise, • its operation affected by high ambient temperature
	Shunt [86]	• wider torque and speed, • able to run at a predetermined speed, • low-cost power supply	• cannot work at low speed, • expensive, and unreliable at low speeds operations, • the size is large compared with AC motors, and noise
	Series [87]-[89]	• high starting torque, • has more power, • series-wound motors known as universal motors can use for AC or DC supply	• speed control and regulation are not good, • noise, • needs a load before starting
	Compound wound [90], [91]	• quick start and stop, • fast reversing and acceleration	• Operation and maintenance are costly.
	Separately excited [79]	• the stable condition with any field excitation and gives a wide range of output speed, • the field can be connected to a constant voltage source to ensure full torque is available at all speeds	• expensive, • more terminals in the terminal box, • dual supply
Stepper Motor [98]-[102]		• run a wide range of speeds, including very slow speeds without reduction gearing, • high start, stop, and reverse response, • highly reliable since no brushes or commutator is used, • the control circuit is the simple and low cost	• resonances can occur if not properly controlled, • not easy to operate at extremely high speeds, • it is mainly used for low power applications, • noise and vibration
Induction Motor [110], [111]		• working is effortless and very cheap, • operate in a harsh environmental condition, • the construction is robust, • highly efficient motor, from 85 to 95%, • no brushes, and so no sparks, • significantly less maintenance compared to the DC motor and synchronous motor, • three-phase induction motor is self-starting, • does not require DC excitation like synchronous motors • speed variation from no-load to rated load is significantly less	• low starting torque, • efficiency drops at low loads, • at low loads, the power factor drops to very low values, • single-phase needs self-starting torque, and it uses some auxiliaries to rotate the motor
Synchronous Motor [111], [123]		• runs at a wide range of speeds, • easy to change its speed by varying the supply frequency, • less costly in specific kW and speed ranges • higher efficiencies, especially in low speed • has a wide range of power factors, both lagging and leading. So, it can be used for power factor correction,	• not self-starting. Special methods are adopted to make itself starting, • required frequent maintenance, • need an external DC source for providing excitation, • additional damper winding is necessary, • hunting takes place if the load is changed suddenly

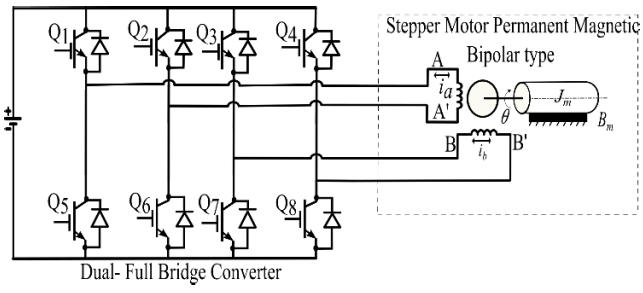

FIGURE 14. Power Circuit of Bipolar PM Stepper Motor Model.

to the ground to allow a unidirectional current flow in each half-coil. This configuration reduces the controlled switches used. However, it reduces the machine torque compared to the bipolar PM-STM working at the same step operation, i.e., full-, half-or micro-step control. Although this circuit is relatively cheaper and easier to control, it has not been used in the heliostat drive system yet as far as the best of the authors' knowledge.

Hence, it is an exciting point to be investigated. A summary of different stepper motors and their power electronic converter circuits are listed in Table 5. and Table 6, respectively.

C. INDUCTION MOTORS DRIVES

Induction motors (IMs) are widely employed in heliostat drive systems and industrial applications. They can produce relatively high torque at low speed, great accuracy, long lifetime, with the availability of several manufacturers in both small and large sizes.

In addition, IMs have higher efficiency than DC motors for the same size and rating, particularly for high ratings, which makes them very suitable for big-size solar tracking

TABLE 6. Typical motors, converter, and application guides.

Type of Drive		Type of power electronic converters	Type of control	Applications
DC Drive [93]-[95]		• thyristor, AC/DC converter	• phase control with inner control loop	• automobiles for operating windshield wipers, • washers, blowers for air conditioners as well as heaters, • food mixers, electric toothbrushes, and moveable vacuum cleaners, • handy electric tools like hedge trimmers, drilling machines, etc. • traction applications, like locomotives, trolley cars, and starter motors in vehicles, • cranes and conveyor belt where higher starting torque is required
		• DC/DC converter (full H-bridge) GTO, IGBT, or MOSFET	• PWM control with internal control loop	• transportation, machine tools, and office equipment. • four quadrants DC drives
Stepper Drive [103]-[104]		• DC/DC converter GTO, IGBT, or MOSFET	• phase current control with PWM	• 3D printing equipment, and printing presses, • automotive gauges and machine tooling automated Production equipment, • medical scanners, samplers, fluid pumps, respirators, and blood analysis machinery, • gaming machines, and small robotics, • CNC milling machines and welding equipment
Induction Drive [111]-[115]	Cage	• back-back thyristor	• phase control	• high torque, and low starting current, such as conveyors, compressors, crushers, agitators, reciprocating pumps
		• IGBT, GTO inverter, or Cycloconverter.	• PWM with *V-f* control	• normal torque and norm starting current, such as fans, blowers, centrifugal pumps, line shafting
		• IGBT, or GTO	• vector control	• high performance, such as sheers, punch presses, die stamping
	Slip ring	• thyristor AC/DC converter	• phase control with DC-link current control	• high torque, medium, and high slip, such as large pumps, fans, shears, punch presses, die stamping
Synchronous Drive [124]-[127]	PM	• IGBT or MOSFET converter	• PWM current control	• the machine tool, small and medium rolling steel equipment, fan, pump, and motion control • light industrial machinery, metallurgy, and mining machinery
	Excited	• thyristor AC/DC converter	• DC-link current control	• large fans, washing machines, refrigerators, air-conditioners, and other household appliances, also use as generators for wind farms and small hydroelectric plants

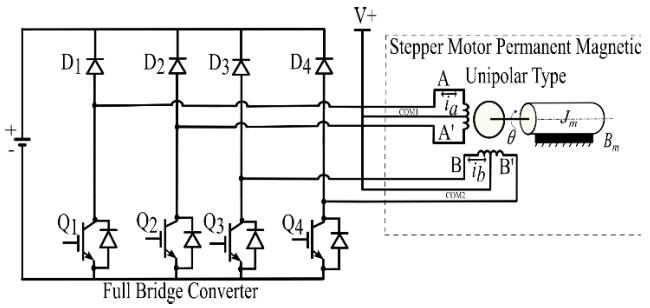

FIGURE 15. Power Circuit of unipolar PM Stepper Motor Model.

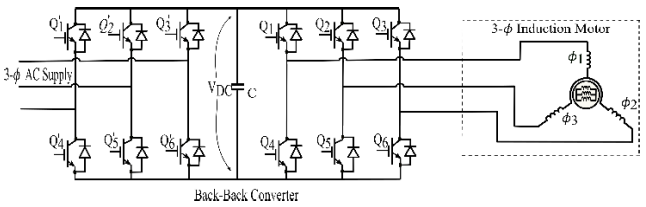

FIGURE 16. Back-to-back converter for three-phase Induction Motor.

systems [36], [105], [106]. Figure 16 shows the typical back-to-back converter used for three-phase IM drives. Variable frequency drive (VFD) and IMs are used together to provide smooth and accurate elevation and azimuthal movements. This method shows a feasible product [107]. A practical solution for double-axis solar tracking applications based on IMs was provided by Siemens [110]. Although the IM and VFD are preferred in industrial applications, the main drawback of this drive system is the difficulty of implementing and justifying the control system compared to DC drives.

Furthermore, for small rating heliostat units using PV as a main supply, it is not easy to get a sufficient DC voltage to supply the IM VFD to drive the IM. Otherwise, an additional boost converter stage has to be added, which is considered an extra cost. The main advantages and drawbacks of the IM drives are listed in Table 5. Furthermore, Table 6 provides a rough guide of combinations of suitable motors and power electronic converters for a few typical applications.

D. SYNCHRONOUS MOTOR DRIVES

For Synchronous motors (SMs), the rotor speed is synchronized with the applied supply speed/frequency, irrespective of the connected load [116], [117]. The stator construction is similar to that of an IM. The difference is in the rotor, which can be a permanent magnet-based rotor or conventional based-field winding rotor [118].

PMSM has many advantages compared to IMs, such as high-power density, high efficiency, high reliability, simple structure, and decreasing the price of permanent magnet materials in recent years. It has become more widely used in various industrial applications [111]. The motor model can be designed with broader air gaps than IMs, which provides more stability. So, the efficiency can exceed 90% [119], [120]. One of the SMs drawbacks is the double excitation for the field-circuit-based type, where a DC source supplies the rotor circuit.

Furthermore, SMs are not self-starting ones, requiring a closed-loop control for starting motor operation at a definite rotor position, which needs shaft encoders that increase the drive system cost [121]. Furthermore, PMSM is a typical nonlinear system with strong coupling and multiple variates. The main challenging factors include current coupling, system saturation, parameter perturbation, and external disturbance [122].

The VFD used for IM can be used for SM drives, which facilitates the speed control of SMs. Although the SMs have better efficiency than IM drives, SMs are considered unsuitable for applications requiring frequent starting or high starting torques needed [122]. Thus, SMs are rarely used in CSP applications. This gap needs to be investigated to improve SM's performance, starting to get the benefits of SM drives in CSP applications.

Further information about the advantages and disadvantages is mentioned in Table 5. Moreover, the different power electronic converters used for SMs are summarized in Table 6.

E. SUMMARY FOR THE ELECTRICAL MOTORS USED IN SPT SYSTEMS

Based on the previous subsections' discussions, the different motors used in SPT systems, the IM is considered the superior motor according to the outstanding advantages compared to others. Additionally, the IM is regarded as the cheapest type according to the markets offering and the mass production [107], [111]–[115]. PM synchronous motors are rarely used in CSP applications as depicted in the different studies and the worldwide implemented plants. This point needs to be investigated to improve the PM synchronous performance and start to get SM drives' benefits in CSP applications. However, the PM motors have the drawback of relatively fast demagnetization of their magnets in particular for such outdoor applications and at high ambient temperature levels, i.e., in Gulf Cooperation Council (GCC) countries [123]–[125]. Therefore, investigating the thermal stress on the PM-based motors is essential.

Regarding the power electronic converters, there are some common advantages and drawbacks for the different power electronic converter according to the basic components, i.e., thyristor, MOSFET, IGBT, and GTO. For instance, the MOSFET and IGBT-based converters, compared to the GTO and Thyristors ones, have faster response and lower losses, particularly at relatively high switching frequencies (several kHz to several hundreds of kHz). Besides, the most recent semiconductor technologies, i.e., the wide-band-gab (WBG) technologies, have lower turn-on and -off transitions. These semiconductor technologies reduce the converter switching losses and allow the converter's operation at high switching frequencies, which greatly impacts the performance of the electrical drives [**?**], [**?**], [134]–[138]. Therefore, the WBG-based electrical drives utilized for SPT need more investigation.

VII. A CASE STUDY FOR DUAL AXES HELIOSTAT TRACKING IN KINGDOM OF SAUDIA ARABIA

A Case study for SPT heliostat CSP topology in Dhahran, Kingdom of Saudi Arabia (KSA), was demonstrated in [138]. A MATLAB code is implemented for the solar position algorithm to calculate the incident angles to track the sunbeams during the year. A drive system composed of two linear actuators, a DC motor-based drive, was developed. A heliostat prototype of an adequate scale is implemented in Dhahran, Saudi Arabia, to validate the theoretical study.

A block diagram for the dual-axis heliostat is shown in Figure 17. It consists of two DC drive systems, i.e., elevation and azimuth drives. Each drive system consists of a linear actuator based on a PMDC motor, and they are supplied from a class-E DC chopper. The model has been validated experimentally using a roof-top heliostat prototype. The experimental platform was tested for several days in different seasons to confirm the prototype capabilities for sun tracking during the year.

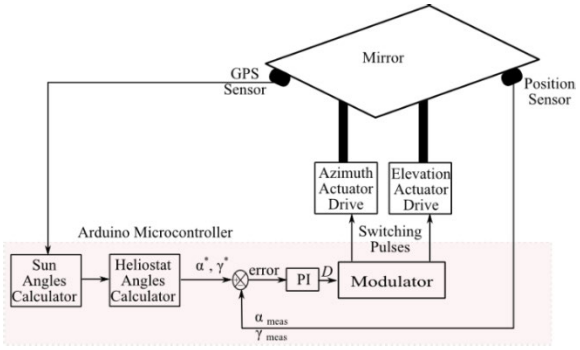

FIGURE 17. Block diagram of dual-axis solar tracking system [138].

To track the sunbeams, three sets of angles, defined in Figure 8-Figure 10, have to be calculated using relations (1)–(6) as a function of time, date, and location. The model converts the sun and tower angles to points and then finds the

normal mirror vector based on three-dimensional Cartesian form. Solar angles for four typical mid-day of the months, July, October, January, and April, represent different seasons. They were simulated based on the longitude of Dhahran, Saudi Arabia. The solar field longitude and latitude are 50.01° and 26.5°, respectively. The solar elevation angle, and the solar azimuth angle, were calculated and plotted for four typical days as explained in Figure 18 and Figure 19, respectively. Considering the heliostat and tower positions, with $\alpha_T = 38.71°$ and $\gamma_T = 170.77°$, the resultant tracking angles are represented in Figure 20 and Figure 21. These figures reflect the long sunny day in this location, which is a good location for CSP applications.

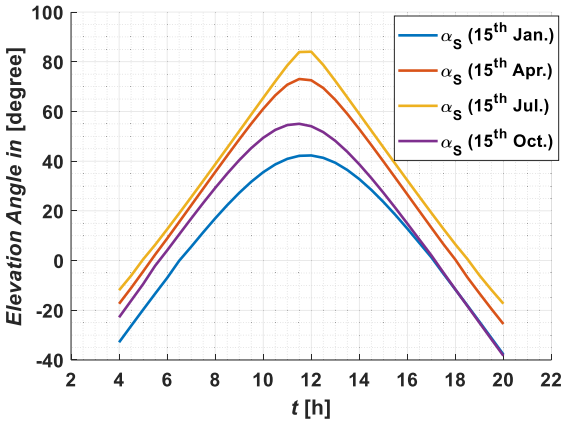

FIGURE 18. Solar elevation angle curves for Dhahran, Saudi Arabia time.

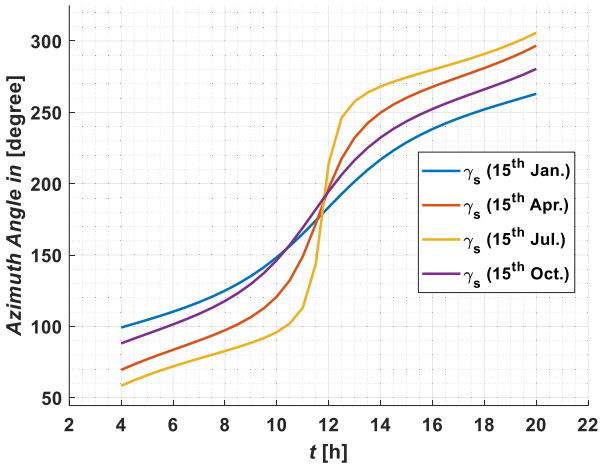

FIGURE 19. Solar azimuth angle curves for Dhahran, Saudi Arabia time.

Experiments have been conducted for several days to evaluate the drive system performance under several conditions. The integrated heliostat prototype is shown in Figure 22-a. The location is the roof-top of an academic building at King Fahd University (KFUPM) in Dhahran, Saudi Arabia. The drive system could reflect the sunbeams accurately, similar to the presented one-day results.

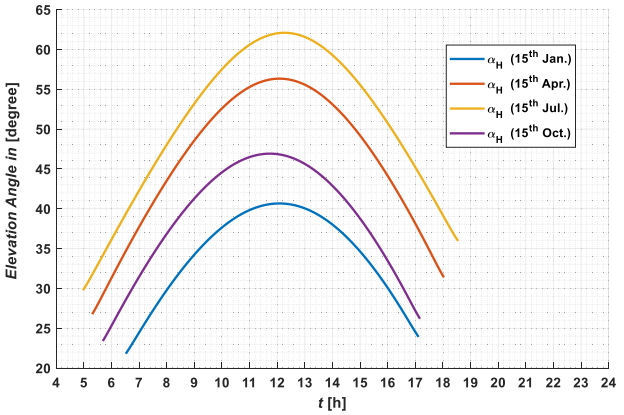

FIGURE 20. Heliostat elevation angle curves for Dhahran, Saudi Arabia time.

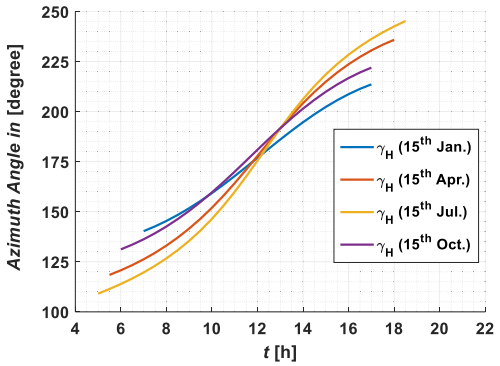

FIGURE 21. Heliostat azimuth angle curves for Dhahran, Saudi Arabia time.

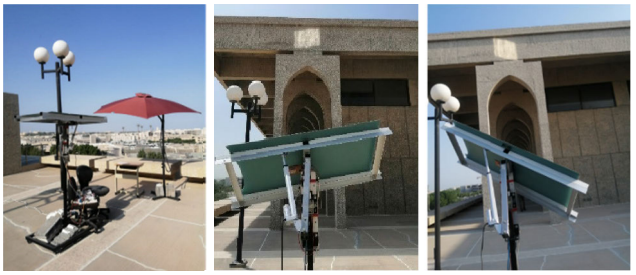

FIGURE 22. The proposed prototype of the automatic dual-axis solar tracking unit.

For instance, one day's experimental results (Jul. 15th, 201) from sunrise to sunset are presented in Figure 23 and Figure 24. These figures represent a comparison between the reference calculated angles and the measured angles. Therefore, the drive system starts moving from the stow-position to the calculated heliostat angles for both azimuth and elevation angles. The tracking system could then follow the reference heliostat angles along the day, as shown in the same figures. By the end of the day, the heliostat drive is returned to the mirror to the stow-position at sunset at 6:30 P.M. The figure reflects that the drive system could follow the reference

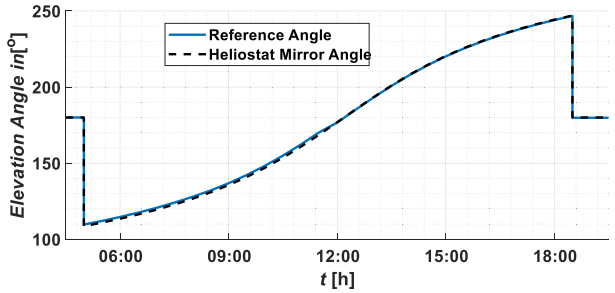

FIGURE 23. Reference and tracking angle for azimuth angle with heliostats mirror angles on Jun. 15th, 2020.

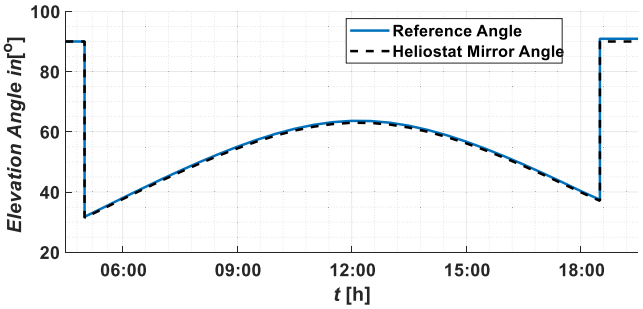

FIGURE 24. Reference and tracking angle for elevation angle with heliostats mirror angles on Jun. 15th, 2020.

angles properly. Figure 22 b & c illustrate the heliostat operation instantly while the mirror reflects the sunbeams to the desired target. The experimental and simulation results were well agreed.

VIII. FUTURE WORK

According to the discussions in this paper, the following topics are considered promising and need more investigation. These are:

- The electrical motor performance is affected by the operating temperatures and weather conditions. Therefore, studying the effect of different weather conditions, particularly the high ambient temperature, should be investigated on the other electrical motors, especially the permanent magnet ones.
- Recently, advanced semiconductors have been invented, such as WBG technologies. These technologies are preferred due to their superior performance in terms of efficiency and fast responses. Therefore, the outdoor CSP WBG-based power electronic converters need to be investigated at the different operating conditions, i.e., normal and abnormal operating conditions.
- The electrical drive needs more investigations for different motor types such as switched reluctance, PMSM, and BLDC motors. Developing resilient drive systems is crucial under harsh weather conditions, similar to that in Saudi Arabia.
- Cheap sensors used for solar tracking control need to be developed to reduce the SPT drive system cost, along with achieving accurate reflection for the heliostat units.
- A communication protocol for an STP plant needs to be developed to reduce communication losses and improve control performance.
- A huge power cabling network is used to supply the SPT heliostat drive systems. Therefore, a sustainable self-supplied heliostat is an excellent solution and needs proper design and investigation.

IX. CONCLUSION

This paper introduced a comprehensive review of the different SPT drive system topologies, performance, and applications. A comparison between the different CSP topologies and corresponding standing projects worldwide has been presented. The advantages of the SPT system in terms of overall efficiency and temperature levels have been demonstrated. The different drive mechanisms, considering the power source and the industrial transmission solutions, have been summarized. It has been concluded that the electrical actuator is preferred compared with hydraulic ones, particularly with small size heliostat units. The different electrical motors and their corresponding power electronic converters used for SPT heliostat have been discussed. The advantages and drawbacks of each electrical drive have been presented. A summary of the electrical motors and the recent advancements of power electronic converter components are discussed. The elevation-azimuth tracking model has been discussed in detail and developed for a dual-axis tracking system based on two linear actuators' drive system. Dhahran KSA is selected, as a promising location for CSP technologies, to test the proposed prototype. The results showed the accuracy of the proposed drive system and validated the use of the azimuth-elevation model for the dual-axis SPT tracking system.

REFERENCES

[1] *Global Energy Transformation: A Roadmap to 2050*, Int. Renew. Energy Agency, Abu Dhabi, United Arab Emirates, 2019.
[2] A. Zervos and R. Adib. Renewables 2019 Global Status Report. REN21. Accessed: 2019. [Online]. Available: https://www.ren21.net/wp-content/uploads/2019/05/gsr_2019_full_report_en.pdf
[3] A. Pfahl, "Survey of heliostat concepts for cost reduction," *J. Sol. Energy Eng.*, vol. 136, no. 1, Feb. 2014, Art. no. 014501.
[4] A. Ummadisingu and M. S. Soni, "Concentrating solar power–technology, potential and policy in India," *Renew. Sustain. Energy Rev.*, vol. 15, no. 9, pp. 5169–5175, 2011.
[5] M. T. Islam, N. Huda, A. B. Abdullah, and R. Saidur, "A comprehensive review of state-of-the-art concentrating solar power (CSP) technologies: Current status and research trends," *Renew. Sustain. Energy Rev.*, vol. 91, pp. 987–1018, Aug. 2018.
[6] Q. Xie, Y. Xiao, X. Wang, D. Liu, and Z. Shen, "Heliostat cluster control for the solar tower power plant based on leader-follower strategy," *IEEE Access*, vol. 7, pp. 135031–135039, 2019.
[7] Y. Hu, Z. Xu, C. Zhou, J. Du, and Y. Yao, "Design and performance analysis of a multi-reflection heliostat field in solar power tower system," *Renew. Energy*, vol. 160, pp. 498–512, Nov. 2020.
[8] S. Shao, X. Zhu, and Y. Fan, "A study on cosine efficiency in a tower reflector solar power system," in *Proc. Chin. Automat. Congr. (CAC)*, Nov. 2019, pp. 4224–4227.

[9] J. C. Sattler, M. Röger, P. Schwarzbözl, R. Buck, A. Macke, C. Raeder, and J. Göttsche, "Review of heliostat calibration and tracking control methods," *Sol. Energy*, vol. 207, pp. 110–132, Sep. 2020.

[10] Y. Xiao, Q. Xie, and Z. Deng, "A review on heliostat field layout and control strategy of solar tower thermal power plants," in *Proc. Chin. Autom. Congr. (CAC)*, Nov. 2018, pp. 1909–1912.

[11] T. M. Pavlović, I. S. Radonjić, D. D. Milosavljević, and L. S. Pantić, "A review of concentrating solar power plants in the world and their potential use in Serbia," *Renew. Sustain. Energy Rev.*, vol. 16, no. 6, pp. 3891–3902, Aug. 2012.

[12] S. Rech, A. Lazzaretto, and E. Grigolon, "Optimum integration of concentrating solar technologies in a real coal-fired power plant for fuel saving," *Energy Convers. Manage.*, vol. 178, pp. 299–310, Dec. 2018.

[13] G. Manente, S. Rech, and A. Lazzaretto, "Optimum choice and placement of concentrating solar power technologies in integrated solar combined cycle systems," *Renew. Energy*, vol. 96, pp. 172–189, Oct. 2016.

[14] A. Ummadisingu and M. Soni, "Concentrating solar power–technology, potential and policy in India," *Renew. Sustain. Energy Rev.*, vol. 15, no. 9, pp. 5169–5175, 2011.

[15] H. L. Zhang, J. Baeyens, J. Degrève, and G. Cacères, "Concentrated solar power plants: Review and design methodology," *Renew. Sustain. Energy Rev.*, vol. 22, pp. 466–481, Jun. 2013.

[16] Y. T. Chen, K. K. Chong, C. S. Lim, B. H. Lim, K. K. Tan, O. Aliman, T. P. Bligh, B. K. Tan, and G. Ismail, "Report of the first prototype of non-imaging focusing heliostat and its application in high temperature solar furnace," *Sol. Energy*, vol. 72, no. 6, pp. 531–544, Jun. 2002.

[17] H. Muller-Steinhagen and F. Tieb. (2004). *Concentrating Solar Power, a Review of the Technology*. Accessed: May 28, 2020. [Online]. Available: https://www.raeng.org.uk/publications/ingeniamagazine

[18] *IRENA Solar Atlas*. Accessed: Nov. 24, 2020. [Online]. Available: https://solarpaces.nrel.gov-/by-country

[19] C. Lee and L. G. Frechette, "A silicon microturbopump for a rankine-cycle power generation microsystem—Part I: Component and system design," *J. Microelectromech. Syst.*, vol. 20, no. 1, pp. 312–325, Feb. 2011.

[20] J. Zhu and Z. Chen, "Optical design of compact linear fresnel reflector systems," *Sol. Energy Mater. Sol. Cells*, vol. 176, pp. 239–250, Mar. 2018.

[21] N. El-Bassam, P. Maegaard, and M. L. Schlichting, "Distributed renewable energies for off-grid communities, concentrated solar power," in *Renewable Energy and Alternative Technologies, Energy*. 2013, pp. 91–109.

[22] R. I. Dunn, P. J. Hearps, and M. N. Wright, "Molten-salt power towers: Newly commercial concentrating solar storage," *Proc. IEEE*, vol. 100, no. 2, pp. 504–515, Feb. 2012.

[23] D. Beegun, D. Juggurnath, M. K. Elahee, and A. Khoodaruth, "Design of a concentrated solar power hybrid system for electricity production for a textile manufacturing plant," in *Proc. 7th Int. Renew. Sustain. Energy Conf. (IRSEC)*, Nov. 2019, pp. 1–6.

[24] Y. T. Chen, K. K. Chong, C. S. Lim, B. H. Lim, K. K. Tan, O. Aliman, T. P. Bligh, B. K. Tan, and G. Ismail, "Report of the first prototype of non-imaging focusing heliostat and its application in high temperature solar furnace," *Sol. Energy*, vol. 72, no. 6, pp. 531–544, Jun. 2002.

[25] H. Müller-Steinhagen and F. Trieb, "A review of concentrating solar power technology," *Ingenia*, vol. 18, pp. 43–50, Mar. 2004.

[26] O. López, J. F. Sáez, A. Baños, and A. Arenas, "Modeling and control of steam generation with a parabolic dish collector," in *Proc. 5th Int. Conf. Event-Based Control, Commun., Signal Process. (EBCCSP)*, May 2019, pp. 1–4.

[27] A. Poullikkas, I. Hadjipaschalis, and G. Kourtis, "The cost of integration of parabolic trough CSP plants in isolated mediterranean power systems," *Renew. Sustain. Energy Rev.*, vol. 14, no. 5, pp. 1469–1476, Jun. 2010.

[28] *NREL Database, Crescent Dunes Project*. Accessed: Aug. 20, 2020. [Online]. Available: https://www.nrel.gov/csp-/solarpaces/index.cfm

[29] D. G. Cacuci, *Handbook of Nuclear Engineering*. New York, NY, USA: Springer, 2010.

[30] P. J. Zucatelli, L. Salvalaio, A. L. Pereira, and A. P. Meneguelo, "Energia distribuída proveniente da concentração de energia solar nas universidades do Brasil: Um estudo de caso," *Latin Amer. J. Energy Res.*, vol. 4, no. 2, pp. 11–22, Mar. 2018.

[31] E. Bellos and C. Tzivanidis, "Assessment of linear solar concentrating technologies for Greek climate," *Energy Convers. Manage.*, vol. 171, pp. 1502–1513, Sep. 2018.

[32] A. P. Gonzalo, A. P. Marugán, and F. P. G. Márquez, "A review of the application performances of concentrated solar power systems," *Appl. Energy*, vol. 255, Dec. 2019, Art. no. 113893.

[33] J. N. Larmuth, "Heliostat cost reduction methods applied to a small heliostat," M.S. thesis, Dept. Mech. Eng., Univ. Stellenbosch, South Africa, Dec. 2015.

[34] Y. Li and T. Takahashi, "Power transfer system with reduced component ratings," U.S. Patent 2004/0 095 789 A1, May 20, 2004.

[35] U. Jakobsen, K. Lu, P. O. Rasmussen, D.-H. Lee, and J.-W. Ahn, "Sensorless control of low-cost single-phase hybrid switched reluctance motor drive," *IEEE Trans. Ind. Appl.*, vol. 51, no. 3, pp. 2381–2387, May 2015.

[36] A. Pfahl, M. Randt, C. Holze, and S. Unterschütz, "Autonomous lightweight heliostat with rim drives," *Sol. Energy*, vol. 92, pp. 230–240, Jun. 2013.

[37] K. Mabusela, C. P. Kruger, B. J. Silva, and G. P. Hancke, "Design of a wireless heliostat system," in *Proc. AFRICON*, Addis Ababa, Ethiopia, Sep. 2015, pp. 1–5.

[38] T. Arrif, A. Benchabane, M. Germoui, and B. Bezza, "Optimisation of heliostat field layout for solar power tower systems using iterative artificial bee colony algorithm: A review and case study," *Int. J. Ambient Energy*, vol. 42, no. 1, pp. 65–80, 2021.

[39] F. Téllez, M. Burisch, M. Sánchez, C. Sansom, P. Kirby, P. Turner, C. Caliot, A. Ferriere, A. Bonanos, C. Papanicolas, A. Montenon, R. Monterreal, and J. Fernández, "State of the art in heliostats and definition of specifications—Survey for a low-cost heliostat development," *Sci. Technol. Alliance Guarantee Eur. Excellence Concept Sol. Thermal Energy*, p. 61, Jul. 2017.

[40] B. Ding, A. Plummer, and P. Iravani, "A study of a compliant hydraulic actuator for running robots," in *Proc. Global Fluid Power Soc. PhD Symp. (GFPS)*, Samara, Russia, Jul. 2018, pp. 1–6.

[41] M. Blejan, I. Ilie, R. Radoi, and C. Cristescu, "Electro-hydraulic linear actuator," in *Proc. 39th Int. Spring Seminar Electron. Technol. (ISSE)*, May 2016, pp. 462–467.

[42] C. Bruzzese, M. Rafiei, S. Teodori, E. Santini, T. Mazzuca, and G. Lipardi, "Electrical, mechanical and thermal design by multiphysics simulations of a permanent magnet linear actuator for ship rudder direct drive," in *Proc. AEIT Int. Annu. Conf.*, Cagliari, Italy, Sep. 2017, pp. 1–6.

[43] L. Pugi, G. Pallini, A. Rindi, and N. Lucchesi, "An hydraulic test rig for the testing of quarter turn valve actuation systems," in *Proc. IEEE/ASME 10th Int. Conf. Mech. Embedded Syst. Appl. (MESA)*, Senigallia, Italy, Sep. 2014, pp. 1–6.

[44] R. Ma, F. Zhang, J. Chen, C. Zhang, and X. Sun, "A novel moving coil linear-rotary electromagnetic actuator based on unipolar permanent magnet," in *Proc. IEEE 4th Int. Future Energy Electron. Conf. (IFEEC)*, Singapore, Nov. 2019, pp. 1–5.

[45] L. Xu, M. Lin, X. Fu, and N. Li, "Analysis of a double stator linear rotary permanent magnet motor with orthogonally arrayed permanent magnets," *IEEE Trans. Magn.*, vol. 52, no. 7, pp. 1–4, Jul. 2016.

[46] J. F. Pan, B. B. Yang, W. Jiang, and N. C. Cheung, "Simulation and optimization of a direct drive rotary motor," in *Proc. 5th Int. Conf. Power Electron. Syst. Appl. (PESA)*, Hong Kong, Dec. 2013, pp. 1–4.

[47] L. Xu, M. Lin, X. Fu, and N. Li, "Design and analysis of a double-stator linear–rotary permanent-magnet motor," *IEEE Trans. Appl. Supercond.*, vol. 26, no. 4, pp. 1–4, Jun. 2016.

[48] I. Boldea and S. A. Nasar, "Linear electric actuators and generators," *IEEE Trans. Energy Convers.*, vol. 14, no. 3, pp. 712–717, Sep. 1999.

[49] Y. Yamamoto, K. Kanao, T. Arie, S. Akita, and K. Takei, "Electrical powerless, thermal and optical responsive polymer-based actuator," in *Proc. 18th Int. Conf. Solid-State Sensors, Actuat. Microsyst. (TRANSDUCERS)*, Anchorage, AK, USA, Jun. 2015, pp. 2129–2131.

[50] G. Song, H. Sun, and Y. Zheng, "Study of the control strategy for mechatronics system of electric actuator," in *Proc. Int. Conf. Electr. Mach. Syst. (ICEMS)*, Seoul, South Korea, 2007, pp. 1584–1587.

[51] G. Gruenwald and W. Attride, "A production design concept for electromechanical components," *IRE Trans. Prod. Techn.*, vol. 3, no. 1, pp. 19–25, Apr. 1958.

[52] E. R. Laithwaite, "Rack-and-pinion motors," *Electron. Power*, vol. 16, no. 7, pp. 251–252, Jul. 1970.

[53] B. Su, R. Wang, and S. Hai, "Research on manufacturing of a new bevel gear based on the three-axis CNC bevel gear machine," in *Proc. 2nd Int. Conf. Mech. Automat. Control Eng.*, Hohhot, China, Jul. 2011, pp. 6035–6037.

[54] M. T. Khabou, N. Bouchaala, F. Chaari, T. Fakhfakh, and M. Haddar, "Study of a spur gear dynamic behavior in transient regime," *Mech. Syst. Signal Process.*, vol. 25, no. 8, pp. 3089–3101, Nov. 2011.
[55] O. Baser and E. I. Konukseven, "Kinematic model calibration of a 7-DOF capstan-driven haptic device for pose and force control accuracy improvement," *Proc. Inst. Mech. Eng., C, J. Mech. Eng. Sci.*, vols. 203–210, no. 6, pp. 1328–1340, Jun. 2013.
[56] J. Rens, K. Atallah, S. D. Calverley, and D. Howe, "A novel magnetic harmonic gear," in *Proc. IEEE Int. Electr. Mach. Drives Conf.*, Antalya, Turkey, May 2007, pp. 698–703.
[57] K. Furuta, "Ultra-compact AC servo actuator combining a harmonic drive gear," in *Proc. IEEE Workshop Adv. Robot. Social Impacts*, Tokyo, Japan, Nov. 2009, p. 71.
[58] Z. Hadas and B. Garami, "Mechatronic model of harmonic drive system," in *Proc. 17th Int. Conf. Mechtron., Mechatronika (ME)*, Prague, Czech Republic, 2016, pp. 1–6.
[59] H. Walker, "Improvements in worm gear manufacture," *J. Inst. Prod. Eng.*, vol. 14, no. 11, pp. 587–590, Nov. 1935.
[60] S. Kikuchi and K. Tsurumoto, "Design and characteristics of a new magnetic worm gear using permanent magnet," *IEEE Trans. Magn.*, vol. 29, no. 6, pp. 2923–2925, Nov. 1993.
[61] G.-H. Jang, C.-W. Kim, S.-W. Seo, K.-H. Shin, I.-J. Yoon, and J.-Y. Choi, "Torque characteristic analysis and measurement of magnetic rack–pinion gear based on analytical method," *IEEE Trans. Magn.*, vol. 55, no. 7, pp. 1–5, Jul. 2019.
[62] H. J. Stadtfeld, "The applications of bevel gears," in *Technical, Power Transmission Engineering*. Rochester, NY, USA: The Gleason Works, Dec. 2014.
[63] S. H. Yahaya, M. S. Salleh, and J. M. Ali, "Spur gear design with an S-shaped transition curve application using mathematica and CAD tools," in *Proc. Int. Conf. Mach. Vis.*, Kota Kinabalu, Malaysia, 2009, pp. 426–429.
[64] T. Jiang, L.-J. Li, R.-L. Zhou, and J.-G. Li, "The discussion of spur gear library system based on UG/open," in *Proc. 2nd Int. Conf. Digit. Manuf. Automat.*, Zhangjiajie, China, Aug. 2011, pp. 1266–1269.
[65] F. Sloan, S. Bull, and R. Longerich, "Design modifications to increase fatigue life of fiber ropes," in *Proc. IEEE/MTS OCEANS Conf. (OCEANS)*, Washington, DC, USA, Sep. 2005, pp. 829–835.
[66] S. Kitano, S. Hirose, A. Horigome, and G. Endo, "TITAN-XIII: Sprawling-type quadruped robot with ability of fast and energy-efficient walking," *ROBOMECH J.*, vol. 3, no. 1, Dec. 2016, Art. no. 8.
[67] L. B. Bridgwater, C. A. Ihrke, M. A. Diftler, M. E. Abdallah, N. A. Radford, J. M. Rogers, S. Yayathi, R. S. Askew, and D. M. Linn, "The robonaut 2 hand–designed to do work with tools," in *Proc. IEEE Int. Conf. Robot. Automat. (ICRA)*, Saint Paul, MN, USA, May 2012, pp. 3425–3430.
[68] J. M. Caputo and S. H. Collins, "An experimental robotic testbed for accelerated development of ankle prostheses," in *Proc. IEEE Int. Conf. Robot. Automat. (ICRA)*, Karlsruhe, Germany, May 2013, pp. 2645–2650.
[69] R. Smith and R. K. Mobley, "Chain drives," in *Industrial Machinery Repair*. London, U.K.: Elsevier, 2003, pp. 120–132.
[70] K. Ueura and R. Slatter, "ACTUATORS: Development of the harmonic drive gear for space applications," in *Proc. 8th Eur. Symp. Space Mech. Tribol.*, Toulouse, France, Oct. 1999, pp. 829–835.
[71] P. Folęga and G. Siwiec, "Numerical analysis of selected materials for flexsplines," *Arch. Metall. Mater.*, vol. 57, no. 1, pp. 185–191, Jan. 2012.
[72] M.-W. Park, J.-H. Jeong, J.-H. Ryu, H.-W. Lee, and N.-G. Park, "Development of speed reducer with planocentric involute gearing mechanism," *J. Mech. Sci. Technol.*, vol. 21, no. 8, pp. 1172–1177, Aug. 2007.
[73] M. L. Roderick, "Methods for calculating solar position and day length including computer programs and subroutines," Dept. Agricult. Food, Perth, WA, Australia, Tech. Rep. 137, 1992, p. 81.
[74] M. Debbache, A. Takilalte, O. Mahfoud, H. Karoua, S. Bouaichaoui, M. Laissaoui, and A. Hamidat, "Mathematical modelization of an azimuthal-elevation tracking system of small scale heliostat," *Int. J. Control Theory Appl.*, vol. 9, no. 38, pp. 111–120, 2016.
[75] M. Guo, Z. Wang, J. Zhang, F. Sun, and X. Zhang, "Accurate altitude–azimuth tracking angle formulas for a heliostat with mirror–pivot offset and other fixed geometrical errors," *Sol. Energy*, vol. 85, no. 5, pp. 1091–1100, May 2011.
[76] H. Satpathi, G. K. Dubey, and L. P. Singh, "A general method of analysis of chopper fed D.C. separately excited motor," *IEEE Trans. Power App. Syst.*, vol. PAS-102, no. 4, pp. 990–997, Apr. 1983.
[77] M. R. Erickson and J. A. Kaehler, "Heliostat control employing direct current motor," U.S. Patent 4 536 847, Aug. 20, 1985.
[78] L. Zi-Yi, W. Sew-Kin, P. Wai-Leong, and O. Chee-Pun, "The design of DC motor driver for solar tracking applications," in *Proc. IEEE Int. Conf. Semiconductor Electron. (ICSE)*, Sep. 2012, pp. 556–559.
[79] A. Zeghoudi and A. Chermitti, "Speed control of a DC motor for the orientation of a heliostat in a solar tower power plant using artificial intelligence systems (FLC and NC)," *Res. J. Appl. Sci., Eng. Technol.*, vol. 10, no. 5, pp. 570–580, Jun. 2015.
[80] A. Zeghoudi, A. Chermitti, and B. Benyoucef, "Contribution to the control of the heliostat motor of a solar tower power plant using intelligence controller," *Int. J. Fuzzy Syst.*, vol. 18, no. 5, pp. 741–750, Nov. 2015.
[81] F. Bedaouche, A. Gama, A. Hassam, R. Khelifi, and M. Boubezoula, "Fuzzy PID control of a DC motor to drive a heliostat," in *Proc. Int. Renew. Sustain. Energy Conf. (IRSEC)*, Dec. 2017, pp. 1–6.
[82] J. A. Carballo, J. Bonilla, L. Roca, and M. Berenguel, "New low-cost solar tracking system based on open source hardware for educational purposes," *Sol. Energy*, vol. 174, pp. 826–836, Nov. 2018.
[83] SolarPACES. (2020). *CSP Projects Around the World—SolarPACES*. Accessed: Feb. 24, 2020. [Online]. Available: https://www.solarpaces.org/csptechnologies-/csp-projects-around-the-world
[84] P. Pillay and R. Krishnan, "Modeling of permanent magnet motor drives," *IEEE Trans. Ind. Electron.*, vol. IE-35, no. 4, pp. 537–541, Nov. 1988.
[85] F. N. Klein and M. E. Kenyon, "Permanent magnet DC motors design criteria and operation advantages," *IEEE Trans. Ind. Appl.*, vol. IA-20, no. 6, pp. 1525–1531, Nov. 1984.
[86] J. Chiasson and M. Bodson, "Nonlinear control of a shunt DC motor," *IEEE Trans. Autom. Control*, vol. 38, no. 11, pp. 1662–1666, Nov. 1993.
[87] Z. Xu and Y. Kang, "PWM speed DC motor drive power design," in *Proc. 31st Youth Academic Annu. Conf. Chin. Assoc. Automat. (YAC)*, Wuhan, China, Nov. 2016, pp. 419–423.
[88] D. Zhao and N. Zhang, "An improved nonlinear speed controller for series DC motors," *Proc. IFAC Volumes*, vol. 41, no. 2, pp. 11047–11052, 2008.
[89] Z. Bitar, S. A. Jabi, and I. Khamis, "Modeling and simulation of series DC motors in electric car," *Energy Procedia*, vol. 50, pp. 460–470, Jan. 2014.
[90] H. Oosawa, G. Kimura, M. Shioya, and S. Sano, "Improved resonant type DC/DC converter for control of a compound DC motor," in *Proc. Conf. Rec. Power Convers. Conf., Yokohama*, Yokohama, Japan, 1993, pp. 335–340.
[91] E. Soressi, "New life for old compound DC motors in industrial applications?" in *Proc. IEEE Int. Conf. Power Electron., Drives Energy Syst. (PEDES)*, Bengaluru, India, Dec. 2012, pp. 1–6.
[92] M. H. Rashid, *Power Electronics Handbook: Devices, Circuits, and Applications*. Upper Saddle River, NJ, USA: Prentice-Hall, 2014.
[93] *IEEE Standard Practices and Requirements for Thyristor Converters for Motor Drives Part 1-Converters for DC Motor Armature Supplies*, Standard ANSI/IEEE 444-1973, Jan. 1974, pp. 1–98.
[94] M. Muruganandam and M. Madheswaran, "Performance analysis of fuzzy logic controller based DC-DC converter fed DC series motor," in *Proc. Chin. Control Decis. Conf.*, Guilin, China, Jun. 2009, pp. 1635–1640.
[95] A. Pashaei, M. T. Haque, and S. Alizadeh, "Control of output voltage of simple DC-DC converters," in *Proc. IEEE Vehicle Power Propuls. Conf.*, Windsor, ON, Canada, Sep. 2006, pp. 1–5.
[96] C. W. De Silva, *Sensors and Actuators: Engineering System Instrumentation*. Boca Raton, FL, USA: CRC Press, 2016.
[97] N. Greenough and C. C. Kung, "A new high-efficiency stepper motor driver for old technology stepper motors," in *Proc. IEEE 25th Symp. Fusion Eng. (SOFE)*, Jun. 2013, pp. 1–4.
[98] D. S. Ramteke and M. B. Gaikwad, "Isolated DC-DC converter fed DC motor for bidirectional electric vehicular application," in *Proc. Int. Conf. Smart Electr. Drives Power Syst. (ICSEDPS)*, Nagpur, India, Jun. 2018, pp. 33–37.
[99] H. Moczala, J. Draeger, H. Krauss, H. Schock, and S. Tillner, *Small Electric Motors, Stepper Motors-Principles and Applications*. Stevenage, U.K.: IET, 1998, p. 308.
[100] N. Pitalua-Diaz, V. Benitez, and J. Pacheco-Ramirez, "Stepper motor modeling and control design for a 1.5 square meters heliostat prototype," in *Proc. World Automat. Congr.*, Jun. 2012, pp. 1–6

[101] N. Jirasuwankul and C. Manop, "A lab-scale heliostat positioning control using fuzzy logic based stepper motor drive with micro step and multi-frequency mode," in *Proc. IEEE Int. Conf. Fuzzy Syst. (FUZZ-IEEE)*, Naples, Italy, Jul. 2017, pp. 1–6.

[102] G. Luo, L. Li, J. Wang, W. Wang, J. Song, and Y. Yang, "A heliostat integrated with a sun-position sensor for daylighting," *Energy Procedia*, vol. 158, pp. 394–399, Feb. 2019.

[103] G. Mihalache, A. Zbant, and G. Livint, "Open-loop control of hybrid stepper motor with two phases using voltage to frequency converter," in *Proc. 8TH Int. Symp. Adv. Topics Electr. Eng. (ATEE)*, Bucharest, Romania, May 2013, pp. 1–4.

[104] S. Marhraoui, A. Abbou, N. El Hichami, and S. Rhaili, "Solar MPPT for stepper motor-drive using in industrials applications," in *Proc. Int. Conf. Eng. Technol. (ICET)*, Antalya, Turkey, Aug. 2017, pp. 1–6.

[105] B. Aichi, M. Bourahla, K. Kendouci, and B. Mazari, "Real-time nonlinear speed control of an induction motor based on a new advanced integral backstepping approach," *Trans. Inst. Meas. Control*, vol. 42, no. 2, pp. 244–258, Jan. 2020.

[106] R. Gunabalan, P. Sanjeevikumar, F. Blaabjerg, O. Ojo, and V. Subbiah, "Analysis and implementation of parallel connected two-induction motor single-inverter drive by direct vector control for industrial application," *IEEE Trans. Power Electron.*, vol. 30, no. 12, pp. 6472–6475, Dec. 2015.

[107] J. Enrile, F. Ceron, P. Valera, and R. Osuna, "Prothelios: Heliostat for large PV plants," in *Proc. 3rd World Conf. Photovolt. Energy Convers.*, vol. 3, Osaka, Japan, 2003, pp. 2386–2388.

[108] K. Kurokawa and K. Kato, *Feasibility of Very Large Scale Photovoltaic Power Generation (VLS-PV) Systems*. James & James Ltd, 2003, p. 40.

[109] M. Ito, K. Kato, H. Sugihara, T. Kichimi, J. Song, and K. Kurokawa, "A preliminary study on potential for very large-scale photovoltaic power generation (VLS-PV) system in the Gobi desert from economic and environmental viewpoints," *Sol. Energy Mater. Sol. Cells*, vol. 75, nos. 3–4, pp. 507–517, Feb. 2003.

[110] Siemens. *How to Exploit Sunlight Toward Maximum Energy Yield?* Accessed: Feb. 2020. [Online]. Available: https://eandm.com/media/EandM/PDFs/Siem-ensSolar.pdf

[111] S. Zhang, A. M. Qwbaiban, and T. G. Habetler, "A survey of electric drives for solar tracking control of concentrated solar power heliostats," in *Proc. IECON, 45th Annu. Conf. IEEE Ind. Electron. Soc.*, Lisbon, Portugal, Oct. 2019, pp. 2288–2294.

[112] R. E. Bedford and V. D. Nene, "Voltage control of the three-phase induction motor by thyristor switching: A time-domain analysis using the α–β–0 transformation," *IEEE Trans. Ind. Gen. Appl.*, vol. IGA-6, no. 6, pp. 553–562, Nov. 1970.

[113] B. P. Schmitt and R. Sommer, "Retrofit of fixed speed induction motors with medium voltage drive converters using NPC three-level inverter high-voltage IGBT based topology," in *Proc. IEEE Int. Symp. Ind. Electron. (ISIE)*, vol. 2, Busan, South Korea, Jun. 2001, pp. 746–751.

[114] C. Wang and X. Ma, "Use a less power low voltage IGBT converter to adjust speed of a full power medium voltage induction motor of fan or pump," in *Proc. 4th Int. Power Electron. Motion Control Conf. (IPEMC)*, vol. 2, Xi'an, China, 2004, pp. 664–668.

[115] V. Guennegues, B. Gollentz, F. Meibody-Tabar, S. Raël, and L. Leclere, "A converter topology for high speed motor drive applications," in *Proc. 13th Eur. Conf. Power Electron. Appl.*, Barcelona, Spain, 2009, pp. 1–8.

[116] Z. Wang, S. Li, and S. Fei, "Continuous finite time tracking control for permanent magnet synchronous motor," in *Proc. Int. Conf. Electr. Control Eng.*, Wuhan, China, Jun. 2010, pp. 619–622.

[117] J. R. Xiao and J. F. Pan, "Position tracking control of two permanent magnet linear synchronous motors," in *Proc. 7th Int. Conf. Power Electron. Syst. Appl., Smart Mobility, Power Transf. Secur. (PESA)*, Hong Kong, Dec. 2017, pp. 1–4.

[118] M. Tanaskovic, C. Zhao, F. Percacci, P. Gnos, S. Mariethoz, and D. Frick, "Rotor polarity detection and tracking for slotless permanent magnet synchronous motors," in *Proc. IEEE 9th Int. Symp. Sensorless Control Electr. Drives (SLED)*, Helsinki, Finland, Sep. 2018, pp. 102–107.

[119] R. Shah and R. Gajjar, "A comparative study of various methods for parameter estimation of PMSM," in *Proc. Int. Conf. Energy, Commun., Data Anal. Soft Comput. (ICECDS)*, Chennai, India, Aug. 2017, pp. 1712–1715.

[120] R. Belu, *Building Electrical Systems and Distribution Networks: An Introduction*, vol. 590. Boca Raton, FL, USA: CRC Press, 2020.

[121] S. H. Kim, "Alternating current motors, electric motor control," in *Electric Power—Systems and Networks*. Amsterdam, The Netherlands: Elsevier, 2017, pp. 95–152.

[122] D. Chen, H. Du, and X. Jin, "Position tracking control for permanent magnet synchronous motor based on integral high-order terminal sliding mode control," in *Proc. 32nd Youth Academic Annu. Conf. Chin. Assoc. Automat. (YAC)*, Hefei, China, May 2017, pp. 234–239.

[123] Y. Yang, X. Wang, W. Song, and R. Tang, "Study on the performance sensitivity to ambient temperature for permanent magnet synchronous motor used in pump Jack," in *Proc. 6th Int. Conf. Electr. Mach. Syst. (ICEMS)*, vol. 1, Beijing, China, 2003, pp. 116–119.

[124] D.-W. Kim, D. H. Kang, C.-H. Kim, J.-S. Kim, Y.-J. Kim, and S.-Y. Jung, "Operation characteristic of IPMSM considering PM saturation temperature," *IEEE Trans. Appl. Supercond.*, vol. 30, no. 4, pp. 1–4, Jun. 2020, doi: 10.1109/TASC.2020.2989799.

[125] C. M. Liao, C. L. Chen, and T. Katcher, "Thermal analysis for design of high performance motors," in *Proc. 6th Intersoc. Conf. Thermal Thermomech. Phenomena Electron. Syst. (ITherm)*, Seattle, WA, USA, May 1998, pp. 424–433, doi: 10.1109/ITHERM.1998.689596.

[126] A. Montenon and P. Maussion, "Energy optimization of control loops for concentrated solar plants with the design of experiments," in *Proc. IECON, 39th Annu. Conf. IEEE Ind. Electron. Soc.*, Vienna, Austria, Nov. 2013, pp. 1607–1612.

[127] A. K. Wallace, M. S. Boger, and E. Wiedenbrug, "Medium- and high-voltage, low-speed drives using low-voltage IGBT converters," in *Proc. IEEE Int. Symp. Ind. Electron.*, vol. 1, Dubrovnik, Croatia, Jul. 1995, pp. 86–90.

[128] A. A. Radionov, O. S. Malakhov, S. N. Baskov, A. S. Konkov, and M. S. Davydkin, "The design features of the converters for synchronous motors vector-pulsed launch control," in *Proc. IEEE Region 8 Int. Conf. Comput. Technol. Electr. Electron. Eng. (SIBIRCON)*, Listvyanka, Russia, Jul. 2010, pp. 608–610.

[129] L. Rovere, A. Formentini, G. L. Calzo, P. Zanchetta, and T. Cox, "IGBT-SiC dual fed open end winding PMSM drive," in *Proc. IEEE Int. Electr. Mach. Drives Conf. (IEMDC)*, Miami, FL, USA, May 2017, pp. 1–7.

[130] M. F. Rahman, P. Niknejad, and M. R. Barzegaran, "Comparing the performance of Si IGBT and SiC MOSFET switches in modular multilevel converters for medium voltage PMSM speed control," in *Proc. IEEE Texas Power Energy Conf. (TPEC)*, College Station, TX, USA, Feb. 2018, pp. 1–6.

[131] A. Salem, "Design, implementation and control of a SiC-based T5MLC induction drive system," *IEEE Access*, vol. 8, pp. 82769–82780, 2020, doi: 10.1109/ACCESS.2020.2991691.

[132] M. Fernández, X. Perpina, M. Vellvehi, X. Jorda, J. Roig, F. Bauwens, and M. Tack, "Short-circuit capability in p-GaN HEMTs and GaN MISHEMTs," in *Proc. 29th Int. Symp. Power Semiconductor Devices IC's (ISPSD)*, Sapporo, Japan, May 2017, pp. 455–458, doi: 10.23919/ISPSD.2017.7988916.

[133] A. Salem and M. A. Abido, "T-type multilevel converter topologies: A comprehensive review," *Arabian J. Sci. Eng.*, vol. 44, no. 3, pp. 1713–1735, Mar. 2019, doi: 10.1007/s13369-018-3506-6.

[134] M. Fernández, X. Perpina, J. Roig-Guitart, M. Vellvehi, F. Bauwens, M. Tack, and X. Jorda, "Short-circuit study in medium-voltage GaN cascodes, p-GaN HEMTs, and GaN MISHEMTs," *IEEE Trans. Ind. Electron.*, vol. 64, no. 11, pp. 9012–9022, Nov. 2017, doi: 10.1109/TIE.2017.2719599.

[135] A. Salem, M. Mamdouh, and M. A. Abido, "Predictive torque control and capacitor balancing of a SiC-based dual T-type drive system," *IEEE Trans. Power Electron.*, vol. 35, no. 3, pp. 2871–2881, Mar. 2020, doi: 10.1109/TPEL.2019.2930883.

[136] X. Zhang, G.-S. Qin, and C.-Y. Fan, "The contact type of Ag-GaN piezoelectric semiconductor via experiment," in *Proc. 13th Symp. Piezoelectr., Acoust. Waves Device Appl. (SPAWDA)*, Harbin, China, 2019, pp. 1–4, doi: 10.1109/SPAWDA.2019.8681784.

[137] A. Salem, M. Mamdouh, and M. A. Abido, "Capacitor balancing and common-mode voltage reduction of a SiC based dual T-type drive system using model predictive control," *IEEE Access*, vol. 7, pp. 41066–41077, 2019, doi: 10.1109/ACCESS.2019.2907021.

[138] W. M. Hamanah, A. Salem, and M. A. Abido, "Heliostat dual-axis sun tracking system: A case study in KSA," in *Proc. 18th Int. Conf. Renew. Energies Power Quality (ICREPQ)*, Granada, Spain, Apr. 2020, pp. 1–6.

WALEED M. HAMANAH (Student Member, IEEE) received the B.Sc. degree in electrical engineering from Sana'a, Yemen, in June 2008, and the M.Sc. degree in electrical engineering from the King Fahd University of Petroleum and Minerals (KFUPM), Dhahran, Saudi Arabia, in 2016, where he is currently pursuing the Ph.D. degree in power and machines with the Department of Electrical Engineering. He has worked as an Instructor with Taiz University, Yemen, from September 2008 to December 2011. His research interests include renewable energy, power electronics, machines, and saving energy.

ABOUBAKR SALEM (Member, IEEE) received the B.Sc. and M.Sc. degrees in electrical engineering from Helwan University, Egypt, in 2004 and 2009, respectively, and the Ph.D. degree from Ghent University, Belgium, in 2015. He is currently a Visiting Assistant Professor with the Department of Electrical Engineering, King Fahd University of Petroleum and Minerals (KFUPM). He is involved in several funded projects from KFUPM as a PI and Co-I. He has participated as a Co-I in funded projects from European Union (i.e., STS-Med and Euro-Sun-Med) with a fund of €20 million. His research interests include power electronic converters design and control, electrical drives applications, renewable energy integration, electrical vehicles, and smart grid applications.

M. A. ABIDO (Senior Member, IEEE) received the B.Sc. (Hons.) and M.Sc. degrees in EE from Menoufia University, Shebin El-Kom, Egypt, in 1985 and 1989, respectively, and the Ph.D. degree from the King Fahd University of Petroleum and Minerals (KFUPM), Dhahran, Saudi Arabia, in 1997. He is currently a Distinguished University Professor with KFUPM. He is also a Senior Researcher with the K. A. CARE Energy Research and Innovation Center, Dhahran. He has published two books and more than 400 papers in reputable journals and international conferences. He has participated in more than 60 funded projects and supervised more than 50 M.S. and Ph.D. students. His research interests include power system control and operation and renewable energy resources integration to power systems. He was a recipient of the KFUPM Excellence in Research Award in 2002, 2007, and 2012; the KFUPM Best Project Award in 2007 and 2010; the First Prize Paper Award of the Industrial Automation and Control Committee of the IEEE Industry Applications Society, in 2003; the Abdel-Hamid Shoman Prize for Young Arab Researchers in Engineering Sciences in 2005; the Best Applied Research Award of 15th GCC-CIGRE Conference, Abu Dhabi, United Arab Emirates, in 2006; and the Best Poster Award from the International Conference on Renewable Energies and Power Quality (ICREPQ 2013), Bilbao, Spain, in 2013. He has been awarded the Almarai Prize for Scientific Innovation 2017–2018, the Distinguished Scientist, Saudi Arabia, in 2018, and the Khalifa Award for Education 2017–2018, Higher Education, a Distinguished University Professor in Scientific Research, Abu Dhabi, in 2018.

ABDULAZIZ M. QWBAIBAN (Member, IEEE) received the B.S. degree in electrical engineering from the King Fahd University of Petroleum and Minerals, Dhahran, Saudi Arabia, in 2015, and the M.S. degree in electrical and computer engineering from the Georgia Institute of Technology, Atlanta, GA, USA, in 2018, where he is currently pursuing the Ph.D. degree with the School of Electrical and Computer Engineering. In 2015, he was a Planning Engineer with Aramco, Dhahran. Since January 2019, he has been working on design optimization of induction machines used for concentrated solar power plants with the Electric Power Group, Georgia Institute of Technology. His research interests include design, control, and optimization of electric machines, cybersecurity, and machine learning applied to energy systems.

THOMAS G. HABETLER (Fellow, IEEE) received the B.S.E.E. and M.S. degrees in electrical engineering from Marquette University, Milwaukee, WI, USA, in 1981 and 1984, respectively, and the Ph.D. degree from the University of Wisconsin–Madison, in 1989. From 1983 to 1985, he was employed by the Electro-Motive Division, General Motors, as a Project Engineer. Since 1989, he was with the Georgia Institute of Technology, Atlanta, GA, USA, where he is currently a Professor of electrical and computer engineering. His research interests include electric machine protection and condition monitoring, and switching converter technology and drives. He has published more than 300 technical articles in the field. He is a regular Consultant to the industry in the field of condition-based diagnostics for electrical systems. He was an inaugural recipient of the IEEE-PELS Diagnostics Achievement Award. He was a recipient of the EPE-PEMC "Outstanding Achievement Award," the 2012 IEEE Power Electronics Society Harry A. Owen Distinguished Service Award, and the 2012 IEEE Industry Application Society Gerald Kliman Innovator Award. He has also received one transaction and four conference prize paper awards from the Industry Applications Society. He has served on the IEEE Board of Directors as the Division II Director, and on the Technical Activities Board, a Member and Geographic Activities Board as the Director of the IEEE-USA, and is the Past President of the Power Electronics Society. He has also served as an Associate Editor for the IEEE TRANSACTIONS ON POWER ELECTRONICS.